





Strategies for cell cycle control

Mattia Corigliano¹ , Marco Cosentino Lagomarsino^{1,2} , Jacopo Grilli³ , and Gabriele Micali⁴ 

¹ IFOM ETS, the AIRC Institute of Molecular Oncology, Milan, Italy ; ² Dipartimento di Fisica, Università degli Studi di Milano, and I.N.F.N, via Celoria 16 Milano, Italy; ³ The Abdus Salam International Centre for Theoretical Physics (ICTP), Trieste, Italy; ⁴ IRCCS Humanitas Research Hospital, Rozzano, Milan, Italy

Abstract

Cells require coordination of growth and division, as well as coordination of cell-cycle progression with several essential sub-tasks, such as chromosome replication and segregation. Single-cell dynamics data offer correlation patterns that can be used to understand these decisional processes. The cell-cycle progression and cell-division decisional process can be described by continuous-time and discrete-time stochastic processes. There are quantitative relationships that connect growth, cell-cycle progression, and resource allocation. There are differences and common points in the decisional processes by which single cells of different organisms commit to divide (sizers, adders, accumulators, titration-dilutors, etc.)

Keywords: cell cycle - cell division control - chromosome replication - stochastic process

Contributions: This chapter was drafted and written by Marco Cosentino Lagomarsino, with the help of the other authors. All the authors wrote the introduction and discussion sections (14.1 and 14.7). Mattia Corigliano drafted section 14.5, Marco Cosentino Lagomarsino drafted sections 14.2 and 14.6, Jacopo Grilli drafted section 14.3, Gabriele Micali drafted section 14.4. Michela Pauletti redrew most of the figures. We thank Andrea De Martino for proof correction and feedback on our manuscript.

To cite this chapter: M. Corigliano, M. Cosentino Lagomarsino, J. Grilli, and G. Micali. Strategies for cell cycle control (Version July 2025). doi: [10.5281/zenodo.8156523](https://doi.org/10.5281/zenodo.8156523). Chapter from: The Economic Cell Collective (2025). Economic Principles in Cell Biology. No commercial publisher | Online open access book | doi: [10.5281/zenodo.8156386](https://doi.org/10.5281/zenodo.8156386)

The authors are listed in alphabetical order.



This is a chapter from the open textbook “Economic Principles in Cell Biology”.
Free download from principlescellphysiology.org/book-economic-principles/.
Lecture slides for this chapter are available on the website.



© 2025 The Economic Cell Collective.
Licensed under Creative Commons License CC-BY-SA 4.0.
An online open access book. No publisher has been paid.
doi: [10.5281/zenodo.8156386](https://doi.org/10.5281/zenodo.8156386)

Chapter overview

- Cells require coordination of growth and division, as well as coordination of cell-cycle progression with several essential sub-tasks, such as chromosome replication and segregation.
- Single-cell dynamics data offer correlation patterns that can be used to understand these decisional processes.
- The cell-cycle progression and cell-division decisional process can be described by continuous-time and discrete-time stochastic processes.
- There are quantitative relationships that connect growth, cell-cycle progression, and resource allocation.
- There are differences and common points in the decisional processes by which single cells of different organisms commit to divide (sizers, adders, accumulators, titration-dilutors, etc.)

14.1. Introduction: the decision to divide illustrated through single-cell *E. coli* data.

As nicely put by the Nobel prize winner François Jacob, “the dream of every cell is to become two cells”. Achieving this dream often requires multiple steps, such as growing by a certain size, replicating DNA, and dividing. The previous chapters have addressed cell growth as a consequence of optimization of catabolic and biosynthetic fluxes through optimally regulated resource allocation; this chapter deals with the decision to divide (and to progress the cell cycle), based on growth and other important cellular processes and cues. Clearly this decision to divide or progress the cell cycle must be based on a set of inputs (growth, production processes such as DNA replication and cell-wall biosynthesis, partitioning processes, etc.) and entails several outputs, prominently cell division, but also intermediate key cell-cycle substeps, such as initiation of DNA replication or construction of a “divisome” organelle. The questions that we will consider concern the characterization of the known aspects of this decisional process and its coupling to cell size, to cell growth, and to the chromosome cycle. We will use throughout the chapter *E. coli* as an example. This section provides a description of the main problem through an introduction to the data, based on *E. coli* bacteria. Sections 2-5 start from a mathematical toolbox of models that are useful in this context and compare them with data. Finally, section 6 describes applications to other organisms than *E. coli*.

Capturing the key processes regulating cell division is a fundamental question in biology, which remains open despite a history of more than 60 years. During the years, scientists have learned a great deal about the size and shape of bacteria in different nutrient conditions, what most of the molecular players involved in the division process are, how the DNA replication machinery is formed and how it proceeds along the chromosome, how the septum and the new cell wall are synthesized. However, the vast majority of these data are based on population averages, out of which it turns out to be impossible to extract any direct and/or causal link between the different processes involved in cell growth that set cell division [1]. Today, a new generation of data has the potential to answer several open questions [1, 2, 3]. These data differ from the previous generation in the ability to measure single bacterial cells over multiple division events in controlled conditions. At the same time, the expression of a specific gene or the concentration of specific proteins of interest can be monitored using fluorescent reporters. For example, fluorescent tags on the proteins involved in replication are used to score the initiation of replication in each cell cycle. Single-cell data allow for validating mathematical models and thus bring insights into the causal link between the several processes a cell need to complete before dividing.

By following lineages of cells over multiple generations under controlled environmental conditions, scientists collected different important pieces of evidence (Figure 14.1): First, within a cell cycle, the cell size $s(t)$ is well-described by a single exponential in time¹ [6, 7]: $s(t) = s_0 \exp(\alpha t)$, where s_0 is the size at birth, α is the growth rate, and t is the time since cell birth.

If division occurs at time τ_d , a simple relationship connects the size at division s_d with the other cell properties:

¹Note that most of the studies today use cell length as a proxy for size. However, different choices are possible such as volume or mass, and the differences are not fully characterized [4, 5].

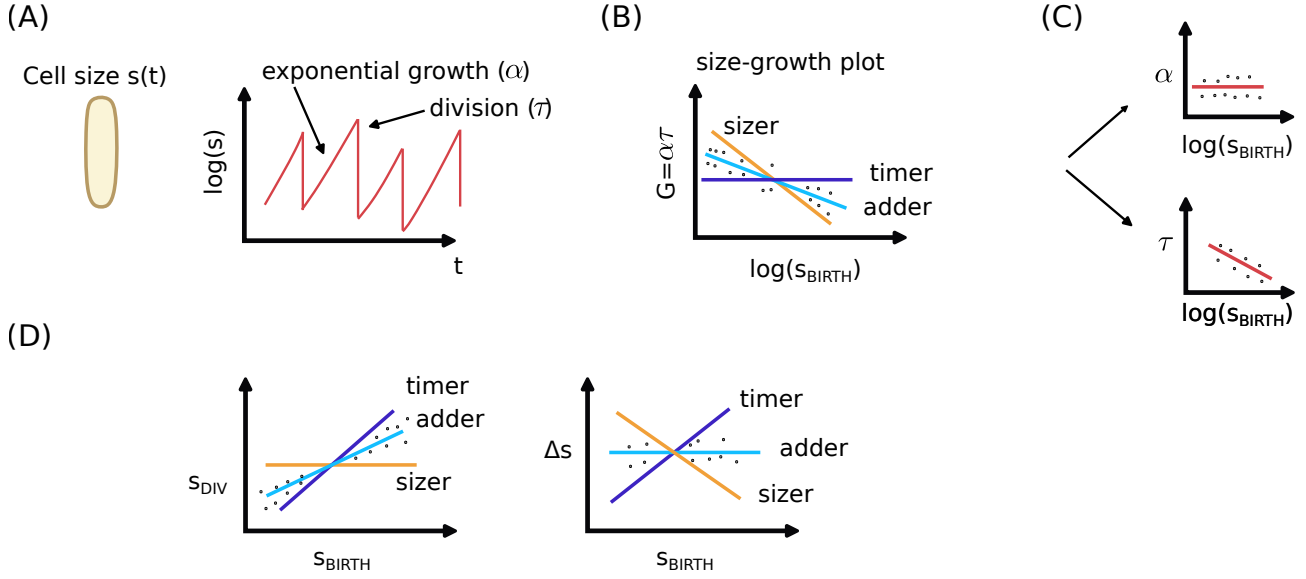


Figure 14.1: Salient quantitative features of cell-division control, explained through *E. coli* data – (A) *E. coli* cells are rod-like. Within a condition they grow by increasing their length, and they divide symmetrically. Following single-cell lineages, growth in length or volume is close to exponential. (B) Size-growth plots quantify the strength of division control. For a timer, multiplicative growth quantified by $G = \log(s_d/s_0)$ is uncoupled to birth size, for a sizer, it is maximally coupled. The single-cell data show an intermediate trend. (C) Since $G = \log(s_d/s_0) = \alpha\tau$, the size-growth plot can be split into contributions correlating birth size to growth rate (top) and/or interdivision time. The data show that *E. coli* bacteria only compensate by modulating interdivision times. (D) Two equivalent quantifications of the strength of the division control size. The intermediate control strategy adopted by *E. coli* adds a size that is independent from the initial size (“adder”). This strategy is sufficient to achieve size homeostasis.

$s_d = s_0 \exp(\alpha\tau_d)$. All the four parameters of this equation are subject to stochasticity in time and vary across single cells, even when they grow in controlled conditions. Second, in steady growth, the size distribution of newborn cells does not change over time, an observation that is referred to as cell-size homeostasis [4]. Equivalently, cells show specific correlation patterns between size at growth and size at division, which are related to their cell-division strategy [8, 4].

Let us try to understand more in detail how single-cell correlation patterns can be used to understand cell-division behaviors. The observation of near-exponential growth immediately suggests a change of variables that is useful to formulate mathematical models and to understand how single cells control cell division. Indeed, if we can assume that growth is exponential, we can use logarithmic sizes instead of linear sizes. One robust observation, is that the elongation $G = \log(s_d/s_0) = \alpha\tau$ depends on the size at birth s_0 (Figure 14.1B). This allows us to generate so-called “size-growth” plots (Figure 14.1B), in which the log-multiplicative growth during a cell cycle of a single cell is plotted as a function of the logarithmic size at birth [8]. Different mechanisms of size control predict different slopes for this plot. A cell division set by a “timer”, for instance, would predict no relation between G and size. Since $G = \log s_d - \log s_0$, if instead $\log s_d$ were independent of the initial size, a “sizer”, one would predict a slope = -1. The *E. coli* data typically fall half way in between these two predictions, a negative slope of about 0.5 (Figure 14.1B).

By noticing that the overall logarithmic growth G during a cell cycle is the product of the single-cell growth rate and inter-division time ($G = \alpha\tau$), we can ask the question of which one of these variables is responsible for the correlation. This analysis disentangles the contributions to cell division control due to growth rate and inter-division timing (Figure 14.1C). In other words, the dependency of G on initial size can be further decomposed on the dependency of growth rate α and division time τ . In *E. coli*, when growth rate and interdivision times are plotted separately as a function of the logarithmic size at birth, the negative slope is only observed in the interdivision-time plot, suggesting that cell control size by adjusting the single-cell interdivision time rather than their single-cell growth

rates. Hence, *E. coli* data indicate that τ does depend strongly on initial size, while the growth rate has only a weak dependency [7].

One can visualize and quantify the mutual dependencies between cell sizes and growth properties in other equivalent ways (Figure 14.1D). For example, in *E. coli* data, the scatter plot relating size at division in the y-axis to size at birth in the x-axis for single cells has a slope of around 1 (and once again this observation holds true for different strains and under different environmental conditions). In this plot, a slope of 0 would suggest that cells on average need to reach a threshold in size upon division, a sizer. More technically, the division size s_d is independent on the initial size s_0 in the case of a sizer. Instead, a slope of 2 in this plot would suggest that cells on average need to wait a fixed time upon division, a timer. The observed intermediate slope of 1 can also be understood using the equivalent plot in which the added size between birth and division is used on the y-axis, studying the dependency of the added size $s_d - s_0$ on s_0 . This latter way to plot the data is particularly popular, given that, for many datasets it shows no dependency, suggesting that adding a constant added size is the mechanism of size control effectively in place. Indeed, for *E. coli* the experimentally observed slope is always close to 0 [9, 10, 4], an observation that goes under the name of “adder” behavior since cells appear to add on average a constant size during the cell cycle (Figure 14.1(B,D)).

It is fairly simple to rationalize why, for exponentially growing cells, a cell division strategy based on a timer does not achieve a homeostatic size. In order to do this, we can call $q(i) = \log(s_0(i))$ the logarithmic cell size at birth of cell-cycle i , and look at its dynamics through subsequent cell cycles. Since $s(\tau) = s_0 \exp(\alpha\tau)$, and $\langle \alpha\tau \rangle = \log 2$, and assuming that cells divide perfectly in two halves, one immediately gets that

$$q(i+1) - q(i) = \nu(i)$$

where $\nu(i)$ is a zero-average random variable independent for each cell-cycle, arising from the size-independent fluctuations of inter-division times (hence, in technical jargon, we can model ν as a discrete-time Markovian random process). Since the jumps in logarithmic size between subsequent cell cycles are random and independent, cell size at birth makes a discrete-time multiplicative random walk, hence, within a population, the distribution of cell sizes at birth tends to get wider and wider across divisions. The following two sections will explain how size homeostasis can be achieved by size-coupled cell divisions.

14.2. Hazard rate approach to cell division

As we have seen in the previous section, *E. coli* cells grow roughly exponentially. Hence, we can describe their growth by a trajectory for size s (measured as cell mass or volume) of the kind $s(t) = s_0 \exp(\alpha t)$, where t is time from cell birth. While experimentally the growth rate α fluctuates with time, we will neglect its variability and assume for the moment that it is constant. As a consequence, the cell grows as a simple exponential function of time. We will address different hypotheses regarding this point in the later sections.

A simple way to describe the decision processes leading to division (or other cell cycle progression events) is the so-called “hazard rate” model [11, 7, 10]. In this framework, as the cell cycle progresses, each cell has a certain probability to divide, and we call h_d the rate of cell division. In principle, this rate can be a function of many different internal cellular parameters, all the processes that contribute setting cell division. However, since we have in mind experiments measuring cell size versus time and recording cell divisions, the most general “empirically accessible” h_d can depend on s, t, s_0, α with the constraint that $s/s_0 = \exp(\alpha t)$. This means that there can be at most three free parameters. We can also consider simplified models, such as $h_d = h_d(s)$ or $h_d = h_d(s, t)$. Empirically, the lack of correlation between α and birth size suggests a smaller role for this parameter. It is important to realize that this formalism is very powerful, as it can be applied more widely to any sub-cell cycle decision (for example, entry into a specific phase, such as initiation of DNA replication, mitosis, etc.), and to measurements of different relevant

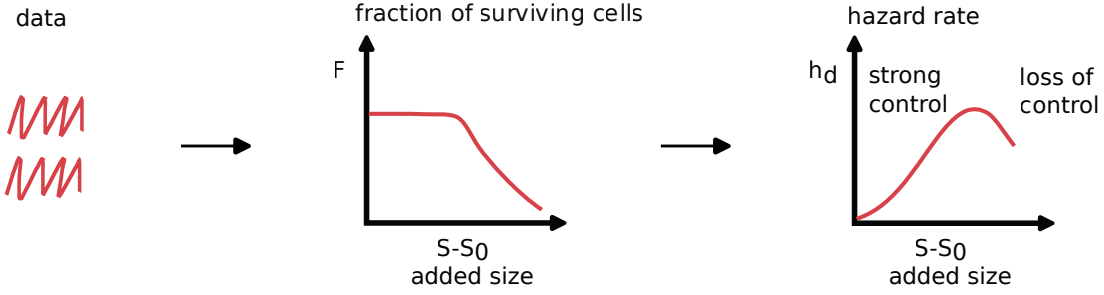


Figure 14.2: Illustration of the inverse hazard rate approach on data – Data from many lineages of dividing cells can be used to estimate the cumulative distribution of non-divided cells, which can also be conditioned on different variables. The drawn example refers to the case where the tested variable is the added size $s - s_0$. In this case, the formalism allows to extract mathematically the hazard rate $h_d(s - s_0)$ from this distribution. Experimental *E. coli* data are consistent with this adder scenario, with an hazard rate that peaks at a characteristic added size, after which the division control weakens.

cell-cycle processes (for example chromosome configurations or the expression of cell-cycle proteins or other factors), which the hazard rate may depend on.

Given a model for the hazard rate, we are interested in the cumulative probability $F(t|s_0, \alpha)$ that a cell born at $t = 0$ has not divided at time t , given that its initial size is s_0 and its exponential growth rate α . Box 14.A discusses the mathematical formalism to obtain this probability.

The considerations we made so far are sufficient to produce “forward models” where a hazard rate is assumed, and one explores its consequences on the division dynamics. The simulation of such a model is straightforward. For each discretized time increment dt , the cell will grow by the prescribed dynamics $s(t)$ and will divide with hazard rate h_d . If a division occurs, the mother’s cell size will halve, and go from s to $s/2$ (we assume for simplicity perfect binary divisions, but this assumption can easily be relaxed). What is a “sizer” in this framework? We can define it as a model where $h_d = h_d(s)$ [12]. Equally, a timer is a model where $h_d = h_d(t)$, and an adder has $h_d = h_d(s - s_0)$. At this stage, it is only intuitive, but not formally grounded, that the scatter plots of the previous section correspond precisely to these models. This problem will be discussed in section 14.3. Note that not all the choices of hazard rates will guarantee a steady-state cell size distribution. As a particular case, one can consider a constant division rate $h_d(t) = r$, which is a simple Poisson process (see the problem above). This is a pure timer and we expect that it will not maintain a steady-state cell size distribution (the reader can verify it, e.g. by simulations).

Beyond the forward approach, we would like to recognize the trends in the data that favor one model rather than another. In particular, we can ask which model best describes the *E. coli* data, presented in the first section of this chapter. This question is a “reverse problem”, and is equivalent to the inference of the hazard rate h_d from data (Figure 14.2). It is a very common reverse problem for the literature, used for example in the so-called “survival analysis” in clinical studies [13]. In that case, the hazard rate typically corresponds to a one-time negative outcome (death of the patient) and the process is not repeated along lineages as in the case of cell divisions. However, the mathematical ingredients are very similar. Consequently, there are many regression methods available in the literature, which can be transferred to our case. One of the most famous is Cox regression [14]. However, most of these regression methods need an ansatz for the parameterization of the model, which might be a nuisance, as it would require some previous knowledge. Here we consider a simpler, direct inference method, which does not need any parameterization (but is effective only with a sufficient amount of data, *i.e.*, for many cell divisions).

Suppose for simplicity we deal with a sizer. In this case, it is possible generate an estimator for the functional form of $h_d(s)$ using Eq. (14.5). By inversion, we obtain

$$h_d(s) = -\alpha s \frac{d}{ds} \log[F(s|s_0)], \quad (14.6)$$

Σ Math box 14.A Probability distribution of (un)divided cells

This box derives the probability distribution of (un)divided cells from the hazard rate. The probability that a cell divides between time t and $t + dt$ is the probability of not having divided so far times the probability of dividing between t and $t + dt$, in turn given by the product of the hazard rate and the time interval dt , $F(t|s_0, \alpha)h_d(s(t), t, s_0, \alpha)dt$. During the same time interval, the cumulative probability of not having divided will decrease by the same amount. Hence, we can write

$$F(t + dt|s_0, \alpha) = F(t|s_0, \alpha)[1 - h_d(s(t), t, s_0, \alpha)dt] . \quad (14.1)$$

In the limit of $dt \rightarrow 0$ we obtain a differential equation, which governs the evolution of our system

$$\frac{d}{dt}F(t|s_0, \alpha) = -h_d(s(t), t, s_0, \alpha)F(t|s_0, \alpha) , \quad (14.2)$$

and whose formal solution is (for $t \geq 0$)

$$F(t|s_0, \alpha) = e^{-\int_0^t dz h_d(s(z), z)} . \quad (14.3)$$

Since we said that the probability of a cell division event in the time interval $[t, t + dt]$ is $P(t|s_0, \alpha)dt = F(t|s_0, \alpha)h_d dt$, the corresponding probability density is

$$P(t|s_0, \alpha) = h_d(s, t)e^{-\int_0^t dz h_d(s(z), z)} = -\frac{d}{dt}F(t|s_0, \alpha). \quad (14.4)$$

Alternatively, the size s can be used as a coordinate, considering for $s > s_0$,

$$F(s|s_0, \alpha) = e^{-\int_{s_0}^s dz h_d^*(z, t(z))} , \quad (14.5)$$

while $F(s|s_0, \alpha) = 0$ for $s < s_0$. Here, $h_d^*(s, t(s))dx$ is the probability of cell division in the size range between s and $s + ds$. The two rates are simply related by $h_d^*(s, t(s))ds = h_d(s(t), s)dt$, where $ds/dt = h_g(s) = \alpha s$ is the rate of growth.

where F can easily be estimated from data, from the cumulative fraction of undivided cells at size s with initial size s_0 . In our case, we can use the mean value of the growth rate $\langle \alpha \rangle$, since we are neglecting fluctuations in growth rate.

Since we do not know whether our assumption of a sizer applies to data, we can first combine the data and the inference to falsify the assumption [7]. In order to do this, we can further condition our histograms in order to fix s_0 . If h_d depends solely on s , then the inferred function \tilde{h}_d should not change with varying s_0 . This is indeed the case if the procedure is applied to simulated data. However, when we apply the same procedure to the experimental data shown in the previous section, the inferred $h_d(s)$ changes if it is inferred for different bins of birth size s_0 . Hence, we conclude that our *E. coli* data do not behave as a sizer, in the sense of the hazard rate. Instead, if we consider the adder ansatz for the hazard rate $h_d(s - s_0)$, and we repeat the procedure, we find that further conditioning by birth size or time from birth does not change our inferred hazard rate [10]. Hence, we can conclude that a hazard-rate analysis of the data supports an adder (or at least that the data cannot falsify this simple model).

How does the inferred h_d depend on size? Curiously, for any fixed s_0 , h_d increases superlinearly for small cell sizes, then reaches a maximum after which it decreases. In other words, some cells may “miss” a cell division event and keep growing until they find a better occasion to divide. This process is called “filamentation” (because the cells that miss one or more division elongate and end up looking like filaments), and is typically the consequence of stress, but also present in stress-free growth conditions. experimental observations show that *E. coli* forms filaments in response to DNA damage, antibiotics, host immune systems, temperature, starvation, and many other stresses. As a

consequence, size plasticity may be in many cases an adaptive strategy. The quantitative division rules of filamentous *E. coli* cells have been studied experimentally [15], but we lack a comprehensive mathematical model.

One very robust observation of cell division statistics, in *E. coli* and beyond [16, 10, 17, 18], is that the distributions of size at birth, size at division, and division times measured across conditions, collapse onto the same curve when rescaled by their mean. For instance, the distributions around these values are clearly non-overlapping: the single-cell birth-size distribution in glucose $p_{glu}(s_0)$ strongly differ from the one in TSB medium $p_{TSB}(s_0)$. In particular, the typical size at birth for *E. coli* growing in glucose $\langle x_0 \rangle_{glu}$ is about 2/3 the size of *E. coli* growing in TSB $\langle s_0 \rangle_{TSB}$ and the average division time $\langle \tau_d \rangle_{TSB}$ is TSB is half the one of *E. coli* in glucose $\langle \tau_d \rangle_{glu}$. This appears to be valid across different environmental conditions (e.g., nutrient quality, temperature, pH, etc.). The remarkable empirical observation is that, when comparing two conditions, the rescaled distribution is universal. If we introduce the rescaled size $\tilde{s}_0 = s_0 / \langle s_0 \rangle_c$, the distribution of \tilde{s}_0 is universal, independent of the condition. This observation applies also to size at division, added size between divisions, interdivision time, and, to a certain extent, growth rate [17].

An obvious question that follows from this observation is how the size-scaling properties of cell-size at birth constrain the mechanisms of homeostasis and the properties of stochasticity at the single-cell level. A necessary consequence of the distribution collapse is that the processes leading to single-cell heterogeneity and homeostasis must have common underlying properties across conditions. Conditions differ because they are characterized by different *dimensional* scales, but, phenomenologically, division control is governed by the same underlying principles (although the key molecular players may vary). The collapse of all the distributions, when the variables are rescaled by the mean has another, stronger, consequence: whatever the division control mechanism is, it depends on only two scales, a size-scale (setting the typical cell size) and a temporal scale (setting growth rate and division time).

This constraint has strict consequences on the variability of the hazard rate across conditions. In particular, it implies that the hazard rate must take the mathematical form [19]

$$h_d(s(t), s_0, t\alpha) = \alpha \tilde{h} \left(\frac{s(t)}{\langle s \rangle_c}, \frac{s_0}{\langle s \rangle_c} \right), \quad (14.7)$$

where the function $\tilde{h}(\cdot, \cdot)$ is the same across conditions. The dependency on α and t disappears, as the scaling of division time, implies the existence of a unique time scale. Since $\tilde{h}(\cdot, \cdot)$ is by definition adimensional, it can only depend on the product αt , which can always be re-expressed as a function of s and s_0 , as $\alpha t = \log(s(t)/s_0)$. While this is a powerful observation, as it allows to naturally connect division mechanisms across conditions, it does not provide any evidence to a particular decisional mechanism enforcing cell division, which is encoded in the function $\tilde{h}(\cdot, \cdot)$. Addressing this question needs further experimental details.

14.3. Cell-division control as a discrete-time linear response process

In the previous section, we have seen how the cell-division control mechanism can be mathematically defined using the hazard-rate framework. This approach uses as a fundamental ingredient the probability per unit time of cell division h_d , which is, *a-priori*, a function of many internal cellular parameters. This approach is, in some sense, very general, as it allows to characterize any complex cellular decision process. However, this generality limits the tractability and interpretability of the model. In this section, we introduce an alternative discrete-time mathematical framework which greatly simplifies the parameterization and the interpretation of a cell-division control model [20, 21], and easily maps to the empirical parameters discussed in Figure 14.1.

Specifically, instead of tracking the division rate at different stages of the cell-cycle, it is often convenient to model directly the cell size at birth across different generations. In this case we can, in full generality, write

$$s_0^{i+1} = f(s_0^i, \alpha, \dots) + \eta^i(s_0^i, \alpha, \dots). \quad (14.8)$$

where s_0^i is the birth size of the cell at generation i . The function $\eta(\cdot)$ represents a random variable whose mean is equal to 0 and having, a priori, arbitrary probability distribution. The function $f(\cdot)$ described the control over cell division. Specifically, the function $f(\cdot)$ can be simply (almost tautologically) defined as the conditional average of the size at birth at generation $i + 1$ given all the variables that contribute to cell division control (the previous size at birth, the growth rate, and others),

$$f(s_0^i, \alpha, \dots) := \langle s_0^{i+1} \rangle_{|x_0^i, \alpha, \dots} . \quad (14.9)$$

The random variable $\eta(s_0^i, \alpha, \dots)$ characterizes the fluctuations around this conditionally averaged birth size.

This formulation of the process is as general as the hazard-rate formalism as it allows to express any division probability $F(s|s_0, \alpha, \dots)$. Eq. (14.8) simply isolates the contribution of the (conditional) average size at division from the deviations from this average. This separation is useful because it allows a clear interpretation of the mechanism of division control, and because the conditional average size at division is typically accessible from single-cell experiments. For instance, a timer corresponds to $f(s_0^i, \alpha) \propto s_0^i$, where the proportionality constant equals $\exp(\alpha\tau_d)/2$. A sizer corresponds to $f(\cdot)$ being a constant, independent of the initial size s_0^i . Along the same lines, an adder is defined as $f(s_0^i, \alpha) = (s_0^i + \Delta(\alpha))/2$, where $\Delta(\alpha)$ corresponds to the (average) added size. The formalism also shows how there is a continuum of possible intermediate behaviors besides these three limit cases.

Given the facts that growth is exponential, and the distribution of sizes at birth is approximately Lognormal [10, 17], it is once again convenient to introduce the logarithmic size $q_0^i = \log s_0^i$. One can derive the dynamics of the variable q_0^i as a function of the dynamics defined in Eq. (14.8) [19]. Since the fluctuations of this variable are small, this dynamics is fully specified by a set of linear-response parameters λ_{ab} relating the main observables (i.e. in our case each of the variables a, b can be q_0, α, τ, G).

The linear-response framework offers a flexible and analytically tractable tool to formulate and explore different models of division control. The models can be constrained by correlation patterns measured in data, quantified for example by covariances, which relate to the coupling parameters λ_{ab} . However, the question remains of whether such models are consistent with data. For *E. coli* data, the linear-response framework predicts the correct consistency relations between experimental measurements, thereby confirming its usefulness to characterize empirical data [21]. A second, more biologically relevant, question is identifying the biological mechanism reproducing the observed dependency patterns. As already discussed, the observation that $\lambda_{qq} \sim 0.5$ is a strong indication of adder-like size-control mechanisms [20, 10, 19, 21]. Interestingly, one can show that the non-zero correlation between growth rate and log-initial size $\langle \delta\alpha^{i+1} \delta q_0^i \rangle$ can be explained because of the correlation between mother and daughter single cell growth rates (the presence of a non-zero value $\lambda_{\alpha\alpha}$ and a dependency of the division size on the growth rate (a non-zero term $\lambda_{q\alpha}$). Such a relation between parameters point to some dependency on the size at division on the single cell-growth rate. For *E. coli*, it is possible [21] to reproduce the empirical values of these coupling parameters by assuming an adder model where the added size depends exponentially on the single-cell growth rate, following the same dependency it has on the population growth rate (this behavior will be discussed in more detail below, and is sometimes termed Schaechter's Law [22]).

14.4. Coordination of cell division with different cell-cycle processes

In the previous sections, we learned that *E. coli* single-cell dynamic data reveal the adder size-control behavior, which allows bacterial cells to maintain size homeostasis. We also discussed a mathematical framework that describes how size control is achieved, and, in particular, how the key measured variables (logarithmic size at birth, interdivision time, growth rate, and total growth during a cell cycle) are connected. Here, we introduce a joint description of the DNA replication cycle, which at the modeling level makes it necessary to partition the cell cycle into sub-periods. We then present the key elements and observations around the debate on whether and how DNA replication and

genome segregation is limiting cell division in *E. coli*. In presenting this debate we aim to (i) highlight the positive and innovative aspects of some of the cornerstone studies of recent years, (ii) provide the reader with robust tools necessary to compare mathematical models against data. Finally, we conclude the section by underlying a few open questions.

It is a classic question in biology [24, 25] how cells achieve the precise coordination of the cell cycle with chromosome replication and segregation is necessary for cell survival. DNA replication defines a way to subdivide the cell cycle into sub-periods. In *E. coli*, the period between cell division and initiation of DNA replication is normally referred as the B-period. The C-period is the period needed to complete replication. Bacterial DNA is organized in circular chromosomes which replicate starting from a well-defined “origin” region (called *ori* locus). The replication machinery moves bi-directionally, and the two “replication forks” proceed approximately at the same speed and terminate in a “terminus” region of the chromosome called *ter* locus [26, 27, 28]. For *E. coli* cells dividing at mean interdivision times from about 20 minutes to about one hour, the replication speed is approximately constant, resulting in an approximately constant C period of around 40 minutes [29]. The D-period is the period that lasts from the end of replication to the next division which thus includes segregation and septum formation. Note that the inter-division time, *i.e.* the time between two consecutive division events, can be as short as 20 minutes in *E. coli*. How can a cell with a division time shorter than the C-period duration have at least two copies of the DNA? Classical studies have shown that *E. coli* and other bacteria can set up multiple overlapping rounds of replication, as summarized by Cooper and Helmstetter in 1968 [25]. For example, a cell at birth is already replicating DNA and has two forks. During the cell cycle, two new initiation events take place, which will only terminate in the daughter cells [30]. We will refer to the “G-period” and the “I-period” as the periods between two consequent division and initiation events, respectively.

As briefly mentioned in the introduction of this chapter, the recent single-cell experiments allow to score initiation and termination of DNA replication by fluorescently tagging proteins involved in the formation of the replication forks or directly the *ori* locus [31, 32, 33, 34, 23]. The scoring of initiation and termination makes it possible to produce the size-growth, and the equivalent adder, plots for any of the sub-periods BCD² as well as for the G- and I-periods (jointly). In the remainder of this section, we will refer to the slope of the size-growth plot of a sub-period X (X = B, C, D, G, or I) as λ_X , and to the slope of the corresponding adder plot as ζ_X . The two slopes are linked by the equation $(1 - \lambda_X) = \frac{\zeta_X + 1}{Q_X}$, where $Q_X = \exp(\langle \text{growth during X} \rangle)$ (see Mathematical Detail Box 14.B).

Having formally defined sub-periods for the cell cycle and the corresponding linear-response formalism, we now proceed by discussing a schematic overview of the experimental observations in *E. coli* that any mathematical model should reproduce:

- The G-period shows an adder behavior, ($\lambda_G = -0.5$, $\zeta_G = 0$) [9, 10].
- The C-period duration is approximately constant across cells and experimental conditions with, a tendency to increase for slow growth rates and the C-period generally shows a timer behavior³ ($\lambda_C = 0$, $\zeta_C = Q_C - 1$) [35, 36, 37, 31, 27].
- The I-period shows an adder behavior, ($\lambda_I = -0.5$, $\zeta_I = 0$) [38, 34, 33].
- The CD-period shows an adder behavior ($\lambda_{CD} = \frac{Q_{CD} - 1}{Q_{CD}}$, $\zeta_{CD} = 0$) [34, 39].
- The single-cell growth rate and the duration of the CD period are inversely proportional [32].

Other interesting observations that are considered in the mathematical models we will present shortly are

- *E. coli* cells divide symmetrically with a narrow distribution of division length with CV = 0.05 [7]. Note that this CV is lower than the CV of both the growth-rate distribution (CV \approx 0.1) and interdivision time distribution (CV \approx 0.2).
- The growth rate of the mother cell is correlated positively with the growth rate of the daughter cells, with a

²Note that under fast-growing conditions the termination is experimentally harder to score reliably and hence in many studies the C and D periods of single cells are considered together as a “CD period”.

³Given the difficulty in observing the C-period in single cells, this last question requires further experimental investigation.

Σ Math box 14.B Linear formalism and adder plots

This box shows how to translate the linear response (“ λ -formalism”) to an equivalent formalism based on the slopes of adder plots (“ ζ -formalism”). The interested reader can find more information in [20, 21, 38, 40, 23]. As discussed previously, Eq. (14.29) makes it possible to estimate the linear-response parameter λ in experimental data from the covariance of log-size fluctuations between subsequent generations, by noticing that $(1 - \lambda_G) = \frac{\langle \delta q_0^{i+1} \delta q_0^i \rangle}{\sigma_{q_0}^2}$, where we refer to λ in Eq. (14.29) as λ_G , to highlight the fact that this equation refers to the G -period. Exponential growth dictates that $2s_0^{i+1} = s_0^i e^{\alpha^i \tau^i}$, where s_0^i , α^i , and τ^i are the size at birth, the growth rate and the interdivision time, respectively. For the cell cycle i one can expand the logarithmic growth $G_G^i := \alpha^i \tau^i$ around its average value ($\langle G_G \rangle \simeq \log 2$) in terms of variations around the logarithmic size at birth $q_0^i := \log s_0^i$. Following this procedure, the cell size at birth of generation $i+1$ within a lineage can be expressed as a function of the parameters of generation i , as follows,

$$2s_0^{i+1} = Q_G (s_0^i)^{1-\lambda_G} \langle s_0 \rangle^{\lambda_G} + \nu_0^i, \quad (14.10)$$

where $Q_G = e^{\langle G_G \rangle} = \exp \langle \log s_d / s_0 \rangle$, s_d is the cell size at division and ν_0^i is a discrete-time Gaussian noise with mean zero and standard deviation σ_{s_0} . Expanding around the average size, for small fluctuations we obtain a mapping between added size and slope of the size-growth plot,

$$\begin{aligned} 2s_0^{i+1} &= Q_G \langle s_0 \rangle + (1 - \lambda_G) Q_G \delta s_0^i + \nu_0^i \\ \delta \Delta_G^i &= [(1 - \lambda_G) Q_G - 1] \delta s_0^i + \nu_0^i. \end{aligned}$$

Here $\Delta_G^i = s_f^i - s_0^i$ is the added size during a cell cycle, and $\delta \Delta_G^i = \Delta_G^i - \langle \Delta_G^i \rangle$ is its fluctuation. Hence, by definition, the term in square brackets must be the slope of the adder plot

$$\zeta_G := (1 - \lambda_G) Q_G - 1. \quad (14.11)$$

Solving the equation for λ_G , we get

$$(1 - \lambda_G) = \frac{(\zeta_G + 1)}{Q_G}, \quad (14.12)$$

which can be used (assuming as usual small fluctuations) to convert the slope ζ_G of the adder plot into the slope of the size-growth plot λ_G , and vice-versa.

Pearson correlation of around 0.5 [6].

The mathematical models proposed in the literature can all be described with the general framework we provided so far. However, they are different in terms of ingredients and relevant variables (Fig. 14.3). Specifically, they can be grouped into two broad classes with fundamentally different views on the role of DNA replication, its impact on cell division control, and ultimately on how the cell division and replication cycles are coupled [40, 41, 27, 33, 34]. A class of ‘replication-centric’ models see the completion of DNA replication as the crucial checkpoint for cell-cycle progression, which fundamentally limits division and initiation events [32, 34]. Instead, ‘replication-agnostic’ models assume that cell division is limited by a cell cycle-related process such as septum or cell wall formation and not by DNA replication [42, 33].

The linear-response theory over sub-periods coupled with the new-generation experimental observations on single cells gives us a powerful tool to compare the different models (see Box 14.C). Crucially, while the slopes of the size-growth plots are ultimately correlation patterns, the interpretation of the *causal* link between them changes across different models. For instance, the replication-centric models generally assume that two parameters among λ_I , λ_B , λ_{CD} are input variables, fixed by an underlying molecular mechanism, while λ_G is an output of the model, *i.e.* an emergent correlation pattern predicted by the model. In contrast, the replication-agnostic models assume a

Σ Math box 14.C Comparing cell-cycle sub-periods models with data

This box describes the quantitative tools necessary to systematically compare cell-cycle sub-periods models with data using the linear-response formalism and size-growth plots. Since the formalism may become very heavy, to avoid complications we will present the case of slow-growth conditions, in which there are no overlapping replication rounds. In addition, we will assume that the growth rate is a constant parameter and we will assume perfectly symmetric division.

Replication-centric models assume λ_{CD} and either λ_B or λ_I to be input parameters in the model. Here, we focus on the case in which λ_{CD}^* and λ_I^* are fixed, which is the case for the Cooper and Helmstetter, Ho and Amir, and Witz et al models [25, 43, 44]. In these models, one has that $\delta q_I^{i+1} = (1 - \lambda_I^*)\delta q_I^i + \alpha \nu_I^i$ and $\delta q_0^{i+1} = (1 - \lambda_{CD}^*)\delta q_0^i + \alpha \nu_{CD}^i$, where q_0^i and q_I^i are the logarithmic sizes at birth and initiation of the cell cycle i , respectively; α is the growth rate, and ν_I^i and ν_{CD}^i are the white noise contribution related to the I and CD periods, respectively. In this class of models, λ_G and λ_B are mathematically linked to λ_{CD}^* and λ_I^* , which provides predictions that can be validated or falsified with data:

$$(1 - \lambda_G) := \frac{\langle \delta q_0^{i+1} \delta q_0^i \rangle}{\sigma_{q_0}^2} = \frac{(1 - \lambda_{CD}^*)^2 (1 - \lambda_I^*) \sigma_{q_I}^2}{\sigma_{q_0}^2}, \quad (14.13)$$

$$(1 - \lambda_B) := \frac{\langle \delta q_I^i \delta q_0^i \rangle}{\sigma_{q_0}^2} = \frac{(1 - \lambda_{CD}^*)(1 - \lambda_I^*) \sigma_{q_I}^2}{\sigma_{q_0}^2}. \quad (14.14)$$

Note that by combining (14.13) with (14.14), we also get the relationship

$$(1 - \lambda_G) = (1 - \lambda_{CD}) (1 - \lambda_B) . \quad (14.15)$$

mechanism for the G-period (λ_G is fixed), and the other correlation patterns are outputs of the model. Hence, the observed relationships between linear-response constants across conditions can be used to select a specific model. In the following, we present replication-agnostic theories first, then replication-centric models, then we introduce a class of models that find a solution of this dichotomy.

The replication-centric models are in line with the classic views on the *E. coli* cell cycle, but they are challenged by recent findings [25, 45, 40, 42, 35]. The 1968 Cooper and Helmstetter model was based only on the available population-average data at that time. The model posits that cell division happens within a defined period (CD) of time after initiation. Shortly after, Donachie [45] combined the Cooper and Helmstetter observation of a constant (population average) CD period with the even older observation that population-average cell size increases with the growth rate with a trend that is compatible with an exponential (Schaechter's law [22], which we mentioned above) and postulated that the population-average mass-per-origins is constant with the growth rate. Crucially, the classic paradigm by which replication limits division rested on indirect conclusions based on population averages, but these assumptions needed to be verified by single-cell data, which showed that things are much more complex [1].

In recent times, Ho and Amir [43] were the first to connect the Cooper-Helmstetter-Donachie ideas with the new observation of adder correlation patterns over the G-period. The authors assumed an adder mechanism during the I-period and a timer mechanism during the CD period. This model produces (in the limit of small noise in the timing of the CD period) an adder behavior in the G-period. Note that in this model $\lambda_I = -0.5$ and $\lambda_{CD} = 0$ are inputs while $\lambda_G \approx -0.5$ is an output of the model. This model, by definition, fails in reproducing the adder behavior in the CD period (which was not known at the time). Although it turned out to be an oversimplification, this work has the merit of connecting the old theories with new single-cell data into a simple and elegant replication-centric model.

The first studies measuring the initiation of DNA replication in single cells [31, 32] brought two new experimental pieces of evidence into the field: they observed the duration of the CD period was inversely proportional to the single-cell growth rate and that the C period does not display any size compensation. Based on their data, Wallden and

coworkers proposed a replication-centric model with a sizer in the B-period ($\zeta_B = -1$), which was later falsified [38, 34, 33]. A subsequent study by a different group [34] measured consecutive initiation events in single cells and observed three adders in the G, I, and CD periods. They then designed an improved version of the Ho-Amir model (already proposed for mycobacteria [46]) in which the initiation of DNA replication triggers both the next initiation and a division event with an adder mechanism. In this model, the adder in the G-period is an output of the model, which emerges from the adder in I and CD when the growth rate is a random variable and a sufficiently skewed asymmetry in cell division is added into the model. This replication-centric model is unable to capture the growth rate CD period inverse relationship discovered by Wallden and coworkers. However, it has the merit of improving the Ho and Amir model accounting for both adders in I and CD and introducing a debate over the importance of asymmetric division.

The replication-agnostic models entered the debate more recently. Based on dynamic cell-wall and cell-geometry measurements, Harris and Theriot proposed a model in which the completion of the division septum, and not the chromosome, was the limiting factor for cell division [41, 42]. This model proposes a simple molecular mechanism for the adder based on three main ingredients: (i) a crucial factor involved in setting division is produced at a rate proportional to the cell size; (ii) this factor needs to reach a threshold in the number in order the cell to divide; (iii) the factor in the next generation has to be reset, with no history dependencies on the previous cell cycle (in the case of the septum, this is natural, as a new septum needs to be produced from zero at every cell cycle). This model structure is still the basis for different mechanistic models explaining the adder during the G period, but the mechanistic factor was also proposed to be a protein [47, 48, 33]. Further evidence in favor of a replication-agnostic view came from experiments performed by the Jun lab [33] aiming to perturb independently the adder correlation pattern in the G-period, while maintaining intact the adder pattern over the I-period, and viceversa. The perturbations were achieved by inducing oscillating levels of the FtsZ protein, which forms a contractile ring structure at the future cell-division site and of the DnaA protein, responsible for the initiation of replication, respectively. The authors interpreted the results of these experiments as a proof that the replication and division cycles are independently regulated, and in particular that completion of DNA replication and segregation is not a limiting factor for cell division. Additionally, the authors re-interpreted the molecular adder model proposed by Harris and Theriot, suggesting that the FtsZ may be the “adder protein” setting division. This work has the merit of providing precious experimental information. However, the model fails to explain the adder behavior over the CD period, as well as the correlation patterns related to how the replication and the division cycles are coordinated [38, 40, 23].

The replication-centric and replication-agnostic views have been firmly opposing each other in recent years (see e.g. [49, 44, 50]). However, a standpoint that is gaining consensus is that neither of these views is able to capture the full complexity of the correlation patterns in the data [38, 40, 23, 35, 27, 51]. The recently proposed “concurrent-cycles” scenario [38, 40, 23] bridges the two opposing views and is in better agreement with the data compared to all the above models. The key innovative element in this theoretical framework lies in the assumption that there is no unique process limiting cell division. Rather a set of competing processes have to be completed before division, and some “downstream control” module (modelled as a logic gate) has to process the input from these processes. In its original formulation [38, 40], based on the available data the competing processes are the DNA replication processes defined by an adder in the I-period, a timer in the replication-segregation period cycle, and a cell division process that adds constant size between two consecutive divisions (division-related cycle). The division is decided by an AND gate, which triggers when both of two actions are completed, the interdivision period is complete and the replication-segregation period is complete. Therefore, the AND gate selects the slowest of the two random processes (which vary across single cells) to set the timing. Note that in this framework the CD period can be set by the intrinsic replication-segregation period of this is the slowest process, or by the interdivision period in case this other process is the slowest one. The concurrent-cycles framework makes precise predictions on how the sub-periods correlations of size change when either the replication-related or the division-related cycles are perturbed. Recently, experiments in which cell wall insertion is delayed confirmed the prediction of the model [23]. Other recent studies proposed similar

frameworks, adding mechanistic details, where the onset of constriction at the divisome [51] and/or a “progression control complex” including the chromosome and the divisome play the role of the gate deciding cell division [35, 27]. Technically, concurrent cycle models need an additional set of parameters compared to the replication-centric and agnostic models (see Box 14.D). These parameters are ultimately summarized by one extra relevant parameter, which can be expressed as the probability that the division-related process sets division (in a given cell cycle). Thus, the replication-centric and replication-agnostic models can be seen as limit cases of the concurrent-cycles framework, where this probability is zero or one respectively.

Despite the large improvement that the concurrent-cycles framework provides in the agreement with data, many questions remain open. For example, we do not know the probability of either of the concurrent processes limiting division varies under different conditions. Recent surveys of the available data [23, 51] suggest that the probability of a chromosome-agnostic cycle increases with increasing growth rate. At very slow growth (interdivision times of 300 minutes or more), it has been suggested that replication-segregation is the limiting process. Additionally, we currently do not know what tunes such probability and what the role of the growth rate may be. We also do not know how many concurrent processes there are and which precisely are the relevant players at the molecular level. Finally, the regulation of initiation of DNA replication could also be set by a “gate” integrating a set of processes, a hypothesis that remains underexplored in the literature.

Σ Math box 14.D The concurrent-cycles framework

This box provides the mathematical relationships that correspond to the ones appearing in Box 14.C for the more general concurrent-cycles framework. Given the complexity of this model, we restrict to the case of no overlapping rounds. In particular, we will show how Eq. (14.15) is no longer valid in the concurrent-cycles framework (without the need to include additional ingredients such as asymmetric division or mother-daughter growth rate correlations).

In the concurrent-cycles model, cell division is determined by the slowest of two processes. The first process is an interdivision, (chromosome-agnostic) cycle that is concluded, for generation i , at a log-size q_H^i , which is expressed as $q_H^i = q_H^* + (1 - \lambda_H^*) (q_0^i - (q_H^* - \log 2)) + \alpha \nu_H^i$, with λ_H size control parameter of this process. The second process is a chromosome replication-segregation cycle (replication-centric), that is concluded, for generation i , at a log-size q_R^i , which is expressed as $q_R^i = q_R^* + \delta q_I^i + \alpha \nu_I^i$. Note that this equation assumes a timer for this process, $\lambda_{CD'}^* = 0$, where CD' identify the time needed for completing DNA replication, which is identical to the measurable CD-period only when this second cycle sets division. The cell size at division is determined by the slowest process, *i.e.* $q_d^i = \max(q_H^i, q_R^i)$. The initiation of DNA replication decides the next initiation independently on the size at birth or division, generating the fluctuation around the logarithmic size at initiation that we already found in Box 14.C, $\delta q_I^{i+1} = (1 - \lambda_I^*) \delta q_I^i + \alpha \nu_I^i$.

To calculate the fluctuations of the logarithmic size at division, we assume that the replication-centric process sets the division of generation i with probability p_H independently on q_0^i and q_I^i . With this assumption, and considering λ_H^* , λ_I^* and $\lambda_{CD'}^* = 0$, the model predicts the following values for the strength of the size-growth plots in the B-, CD- and G-period,

$$(1 - \lambda_B) = (1 - \lambda_{CD}) (1 - \lambda_I) \frac{\sigma_{q_I}^2}{\sigma_{q_0}^2} \quad (14.16)$$

$$(1 - \lambda_{CD}) = (1 - p_H) + p_H (1 - \lambda_H^*) (1 - \lambda_B) \frac{\sigma_{q_I}^2}{\sigma_{q_0}^2}, \quad (14.17)$$

$$(1 - \lambda_G) = (1 - p_H) (1 - \lambda_B) + p_H (1 - \lambda_H^*) \quad (14.18)$$

Overall, the concurrent-cycles model allows to match the experimental trends in the size-growth plots with an additional parameter (p_H). In particular, it allows to break the relationship in Eq. (14.15) without including asymmetric divisions or mother-daughter correlations in growth rates [38, 40, 23].

14.5. Protein sectors and cell division

This chapter focuses on quantitative descriptions of the cell cycle and cell division control, and it is natural to wonder whether and how these considerations relate to the topic of previous Chapters 8 in [52] and 10 in [52] which deal with resource allocation models where cell growth is set by catabolism and biosynthesis. There is a strong link between regulation of growth and cell-cycle progression, which remains a largely open area of investigation both in biology and in quantitative biology / physics of living systems. This section discusses some recent models aimed to describe some specific aspects of the coordination between cell growth and cell-cycle progression. We will start by presenting the main questions that we want to address with the aid of mathematical models. Then we will discuss the main ideas and ingredients behind the models that address these questions, and present some relevant predictions that can be tested and validated against experimental data.

The maintenance of an interplay between cell growth and cell cycle is crucial for the correct functioning of the cell. Specifically, a cell has to adapt both growth and division rates concertedly when either one is perturbed. For example, the response and adaptation to environmental stresses, such as sudden shifts in nutrient conditions or exposure to drugs or toxins, requires the ability to reprogram in a coordinated way cell growth and cell division. Consequently, cells across all kingdoms of life have developed specific mechanisms to precisely coordinate cell cycle progression with cell growth and biosynthesis [53, 54, 4, 55, 8, 56]. There are many mechanisms involved in this coordination, and we lack a complete and coherent quantitative understanding of how this coordination works in different contexts. Sometimes we even lack simple ways to frame questions concerning the effects on cell cycle progression of cell growth perturbations/inhibitions, or the effects of cell growth of cell-cycle perturbations (such as cell cycle arrest).

To formulate and address these questions quantitatively, we would need a theoretical framework where both growth physiology (as in “how does a cell grow?”) and cell-cycle decisions/progression (as in “how does a cell decide when to divide?”) aspects are allowed to play a role and influence each other. However, while both cell growth and cell cycle progression alone have been subject of intense study in the past (especially in bacteria [2], but see ref. [57] for a recent review of these themes in eukaryotes), comparatively little effort has been directed so far toward the development of such unified framework. Nonetheless, recent work has advanced our quantitative understanding of the cross-talk between cell growth and cell cycle progression in bacteria. The remainder of this section will focus on discussing these aspects.

Relatively to the bacterium *E. coli*, recent and current efforts aimed at integrating already existing coarse-grained models of cell physiology and cell cycle control. More precisely, several studies have extended the classic proteome allocation theory, (presented in chapters 8 in [52] and 10 in [52]), which has proven successful in describing several physiological laws, to include also a cell-division proteome sector “ X ”, whose dynamics should implement cell-division control (or cell-cycle progression control) strategies at a phenomenological or molecular level (Fig. 14.4). The current models for *E. coli* usually include a threshold accumulation process for cell division, i.e., proteins of the division sector accumulate during cell cycle progression up to a threshold level that triggers cell division. The previous section has mentioned some candidate molecular players for this accumulation (the FtsZ protein and the cell wall insertion).

Let us take a closer look at the ingredients of this modeling framework. The two main ingredients are (i) the standard proteome allocation theory extended to include a division sector X , alongside to the standard main sectors (see Chapter 8 in [52]), Q (house-keeping), R (ribosomes), P (catabolism and transport), together with (ii) a threshold-accumulation division strategy to set the decision to divide (Fig. 14.4A). Note that the fact that the division factor X is a protein is an implicit assumption in these framework and experimentally things could be more complex. Crucially, the fact that cell division is a proteome sector couples the rates of cellular growth and division, by controlling the synthesis of division proteins. Specifically, the models encode a trade-off between ribosomes and division protein synthesis, which as we will see determines many salient predictions.

Box 14.E shows how these ideas and ingredients can be translated into a mathematical model. The framework that

Σ Math box 14.E A mathematical model

The model consists of two different layers of dynamical equations, and one relationship connecting them. The first set of equations describes cell growth and division as cellular processes

$$\frac{ds}{dt} = \lambda s, \quad \frac{dX}{dt} = k_X s - \frac{d_X}{m_X} X, \quad X(\tau_d) = X_{th} \implies \begin{cases} s(\tau_d) \rightarrow s(\tau_d)/2 \\ X(\tau_d) \rightarrow 0 \end{cases}, \quad (14.19)$$

where cell size s (mass or volume) grows exponentially at a rate λ ($[\lambda] = [T]^{-1}$), while division proteins X , of mass m_X being synthesized and degraded at rates (k_X ($[k_X] = [s]^{-1}[T]^{-1}$), d_X ($[d_X] = [M][T]^{-1}$)), accumulate until a threshold amount of them is reached and cell division occurs, after that cell size is divided exactly in half and division proteins number is reset to zero.

The second set of equations describes the dynamical allocation of the proteome and the biosynthesis layer underlying cell growth, as follows

$$\begin{aligned} \frac{dA}{dt} &= \frac{1}{m_a} \left(k_n P - a k_t R f_a + \sum_{P_i \in \{Q, P, R, X\}} d_{P_i} P_i \right), \\ \frac{dP_i}{dt} &= \frac{1}{m_{P_i}} (a k_t f_{P_i} R f_a - d_{P_i} P_i) . \quad P_i \in \{Q, P, R, X\} . \end{aligned} \quad (14.20)$$

According to Eq. (14.20), free amino-acids (A) are produced from import/catalysis of nutrients at a rate k_n ($[k_n] = [M][T]^{-1}$) per number of catabolic/transport proteins P , and from protein degradation, occurring at a rate $d_{P_i} P_i$ (where d_{P_i} ($[d_{P_i}] = [M][T]^{-1}$) is the degradation rate) for each specific sector. Free amino-acids are taken up to synthesise each proteome sector P_i at a rate equal to the number of active ribosomes ($R f_a$), times the fraction of ribosomes synthesising the specific sector f_{P_i} , times an overall protein translation rate, which in this particular model is equal to a constant translation rate per ribosomes k_t ($[k_t] = [s][T]^{-1}$) times the concentration of free amino-acids $a \equiv (m_a A) / ([a] = [M][s]^{-1})$.

Finally, there must be a connection between the two levels of description, in the sense that cellular rates should be regarded as the result of the underlying biosynthesis dynamics. To make this connection explicit, we write the equation

$$s = \gamma M = \gamma (m_A A + m_P P + m_R R + m_Q Q + m_X X), \quad (14.21)$$

representing mass conservation (if "size" stands for "mass" $s = M$), or the assumption of constant density (if "size" stands for "volume" $s = V$), verified in *E. coli* for population averages but not for single cells, or for certain perturbations [5, 58]. Together, Eqs. (14.19), (14.20) and (14.21) fully specify the model.

we are now going to discuss is consistent with different models recently developed in the literature [59, 60, 61, 62, 55].

In order to exemplify how this framework can generate relevant predictions, we dedicated an appendix "Growth Laws" at the end of this document where some concrete examples taken from the literature are discussed. The mathematical derivations are not exhaustive, but aimed to give the reader a feeling of the "recipe" followed to obtain a given prediction starting from the model's ingredients. The interested reader should have sufficient information to work out the mathematical calculations autonomously or follow the complete derivation in the cited references (for example by Serbanescu et al. [59, 60]).

14.6. Control of cell division across species and kingdoms

The concepts described in the previous sections are widely applicable, but there are many relevant species-specific aspects, so that different crucial assumptions that we have taken so far might break down for different species and kingdoms. Additionally, it should be noted that the approach described here is purely phenomenological, while a biological investigation might be concerned with the detailed molecular players responsible for the cell division and cell-cycle progression decisions. Even in this case, the approach is useful and is being applied in recent work. For

example, if the goal is to understand how the size control phenomenon is regulated, the phenomenological analyses can quantify how the phenomenology of size correction behaves under different mutants and perturbations, helping to identify molecular players and their effects on cell-cycle decisions.

Let us consider briefly some important variations of the approach used so far, relevant for the understanding of different species-specific behaviors. First, it is not granted that single cells grow exponentially, or even that exponential growth is a good approximate description. Even in the cases where exponential growth appears to be a good average description, these averages may emerge from more complex behaviors at the single-cell level or in cell cycle sub-periods. For bacteria, most studies conclude that exponential growth is a sufficiently good description, although recent accounts show deviations [63, 64]. In budding yeast (*S. cerevisiae*), the average growth rate was reported to change at regulatory checkpoints with the cell-cycle phase [65, 66, 67]. In the fission yeast *S. pombe*, a systematic study of single-cell growth concludes that the majority of growth trajectories are best described by a bi-linear growth [68]. In cell lines of animal cells, most studies suggest that, on average, cells grow exponentially until a certain saturation size after which they slow down, but this mean behavior hides many details [4]. For example, it seems that cells in the G1 phase of the cell cycle grow at a slightly slower rate than in later stages of the cell cycle [69].

A second important aspect to consider is whether division is symmetric or not. In *E. coli*, cells divide symmetrically, giving rise to two daughter cells that are nearly equal in size, with a precision of a few percent [7]. However, different species use very different strategies for cell division, which increase variability or explicitly aim for asymmetry. For example, *S. cerevisiae* reproduces through budding (hence the term “budding yeast”). The parent cell creates a small outgrowth that eventually becomes a daughter cell. Both division strategies are common among unicellular organisms (many filamentous fungi grow via budding). Budding creates a parent/offspring distinction in which age-related aspects are not transmitted equally. Since aging may correspond to a decrease in fitness/growth rate, it can also create diversity along lineages. A third important aspect to consider is that the growth rate may be coupled to size and enforce size homeostasis. In other words, homeostasis can be achieved by modulating cell-cycle duration based on size at birth, but also if large-born cells grow slower than small-born ones.

As an example of how different issues can be analyzed with extensions of the phenomenological approaches discussed so far, it is instructive to discuss in more detail how one can use the linear-response framework to detect indications of growth-based size homeostasis. As we mentioned previously, the overall multiplicative growth of a cell in one cycle is quantified by $G = q_f - q_0 = \log \frac{s_f}{s_0} =: \alpha \tau$. The slope λ of the size-growth plot is equivalent to considering the conditional average of G over logarithmic size q ,

$$\langle G \rangle_q = \langle G \rangle - \lambda \delta_q \quad (14.22)$$

As we have seen in Fig 14.1, we can consider the separate contributions of timing and growth to the coupling by taking separate scatter plots with growth rate and cell division time. We can give a more formal quantification of their contributions as follows. We call θ the coupling strength derived from the slope the first plot quantifying control by modulation of interdivision time,

$$\langle \tau \rangle_q = \langle \tau \rangle - \langle \tau \rangle \theta \delta_q, \quad (14.23)$$

and γ the slope quantifying modulation of growth rate based on birth size,

$$\alpha - \langle \alpha \rangle = -\langle \alpha \rangle (\gamma \delta_q) + \nu_\alpha. \quad (14.24)$$

For positive values of γ , cells that are born larger than average can correct their sizes by growing with a slower growth rate, and cells that are born with a smaller size than average can correct by growing at a faster rate. Conversely, for negative values of γ , birth-size related specific growth rate variations increases systematically size variability.

Intuitively, we can understand that θ , γ and λ must be related. First, the overall homeostasis must be the result of

the one enforced by growth-rate modulation and the one enforced by interdivision-time modulation. More formally, the slopes of the correlation plots illustrated in Fig. 14.1 for G , α and τ versus logarithmic birth size must be related, because $G = \alpha\tau$.

Using the linear response approach defined in section 14.3, one can derive the following equation

$$\lambda = \theta\langle\alpha\rangle\langle\tau\rangle + \gamma\langle\alpha\rangle\langle\tau\rangle. \quad (14.25)$$

Eq. (14.25) states that the overall correction to size over a cell cycle has to be the sum of a correction due to modulation of timing and a correction due to the modulation of specific growth rate based on size at birth. For example, if the overall strength is an adder, and the size coupling of the duration of the cell cycle is already an adder, the growth rate must be uncoupled from initial size.

Going back to the data, one can use Eq. (14.25) to evaluate the different strategies, by evaluating the couplings θ , γ and λ from the different scatter plots. Importantly, the constraint imposed by Eq. (14.25) is realized in data from several bacterial species and growth conditions, indicating that the framework is sufficient to describe the data. Work on different bacteria shows widespread adder correlations [2], hence $\lambda \simeq 0.5$. What is more surprising is that adder behavior has been reported for in budding yeast and cultured human cells. Hence, for many species, the inter-division correlation patterns are nearly always close to an adder. One interesting exception is the fission yeast *S. pombe*, discussed below. The widespread adder patterns may suggest common general principles underlying the division control of microorganisms and cultured single mammalian cells. Considering the couplings θ , γ shows a different scenario, with a clear distinction between microorganisms and cultured mammalian cells. In the studied unicellular microbes, the inter-division adder is always due to the modulation of cell-cycle duration. Instead, cultured mammalian cells also rely on growth rate modulation to correct their size. In particular, this rejects the hypothesis that adder behavior may be favored by common underlying mechanisms. Additionally, for budding yeast and mammalian cells, the overall adder behavior emerges from homeostatic regulations acting close to the initiation of replication (G1/S transition) during the cell cycle, and from a weaker regulation of the subsequent parts of the cell cycle [4]. Cell growth outside of G1 is critical in setting the average cell size but appears to be less significant for the size homeostasis effect setting cell-to-cell variability in birth size. This is not the case in bacteria, where we have seen that key questions regarding the specific events in the cell cycle where homeostasis is exerted are still under debate.

The fission yeast *S. pombe* is an interesting case to discuss. This rapidly dividing microorganism is a yeast but uses symmetric division (hence it is sometimes called “fission yeast”), and was the central model system in pioneering studies of the cell cycle. Its size-correction mechanism is the strongest observed in nature, because it can correct size fluctuations in a single cell cycle. Its inter-division size pattern is close to a sizer, but recently the study of mutants with different cell widths has shown that the mechanism that triggers division is based on a surface-area sensor, triggered at a critical cell surface. The molecular effector of this sensing, a protein called Cdr2, has been indentified [70]. Curiously, genetic knockout of this protein does not lead to an ablation of size homeostasis. Rather, fission yeast cells fall back to a volume-based mechanism, suggesting that multiple biochemical circuits play a role in the decision to divide.

Finally, since cells of different species and in different conditions use a range of ways to control cell division, for example sizers or adders. An important question is why a particular species would implement one particular strategy. One possibility is that this trait is under selection, and the fitness of individual cells decreases away from the optimal size. In this case sizers would be favored, because they can compensate for deviations in one cell cycle and minimize fluctuations. A second, more likely, possibility is that intrinsic physiological constraints linking cell cycle and growth are important in determining cell division control. For example, it has been argued that in bacteria size control is a result of a cell's attempt to exert a tight control over the initiation of DNA replication rather than cell division [71].

14.7. Concluding remarks

This chapter focused on modeling the cell cycle. The reader should have acquired an overview of some of the key recent experimental results in this area, as well as the basic mathematical toolbox to address biological questions motivated by single-cell dynamic data, concerning (i) decisional processes during the cell cycle and primarily the decision to divide, (ii) coordination between different cell-cycle processes, and primarily the chromosome cycle with cell division and (iii) the coordination of cell cycle progression with growth.

This chapter is connected with Chapters 8 in [52] and 10 in [52] describing resource allocation models used here to describe growth, and with Chapter 12 in [52], describing models of growth rate variability, because it provides a framework to include a description of the division rate variability.

Problems

Problem 14.1

Show that for cells that grow linearly in time an adder and a timer are the same.

Problem 14.2

Analyze the consequences of a constant per-size hazard rate $h_d^* = 1/\tilde{s}$ and compare them to the consequence of a constant per-time $h_d = r$ (a Poisson process).

Problem 14.3

Analyze the forward hazard rate model for cell division where $h_d(s) = (s/\tilde{s}^2)$ by simulation and/or analytical calculations.

Problem 14.4

Find the hazard rate corresponding to the process defined by appendix Eq. (14.29).

Problem 14.5

Write an explicit expression of the four parameters λ_{ab} appearing in appendix Eqs (14.32) and (14.31) as a function of the covariances between the fluctuations of growth rates and log-size at the same or different generations.

Problem 14.6

Prove that the adder strategy rapidly achieves cell size homeostasis (that is, a controlled cell size at birth) after a few cell generations, independently of the starting initial size. Prove that convergence to homeostasis and loss of memory of the initial cell size is exponential in the number of cell cycles. Write down a simple numerical code to simulate this process and verify your analytical predictions. What is the role of noise in setting the inter-division added size?

Problem 14.7

Write the equivalent of Eq. (14.29) for the I-period and for sub-periods B and CD, and prove the following relationships:

$$(1 - \lambda_I) = \frac{\langle \delta q_I^{i+1} \delta q_I^i \rangle}{\sigma_{q_I}^2}, \quad (1 - \lambda_B) = \frac{\langle \delta q_I^i \delta q_0^i \rangle}{\sigma_{q_0}^2}, \quad (1 - \lambda_{CD}) = \frac{\langle \delta q_0^{i+1} \delta q_I^i \rangle}{\sigma_{q_I}^2},$$

where the log-size fluctuation at initiation for the cell cycle i is $\delta q_I^i := q_I^i - \langle q_I \rangle \approx \log(s_I^i / \langle s_I \rangle)$, with s_I^i the cell size at initiation.

Problem 14.8

Write the equivalent of Eq. (14.12) for the I-period and for sub-periods B and CD.

Problem 14.9

Write the predicted λ_G and λ_I for a model in which λ_{CD}^* and λ_B^* are input parameters of the model. Does Eq. (14.15) still hold?

Problem 14.10

Extend the models in Box 14.C for:

- (a) Overlapping rounds of DNA replication. This case is more difficult to address analytically, but can be easily simulated.
- (b) The ζ -formalism (without overlapping rounds). Use the model to answer the question: can an adder in the I- and CD-period provide the adder behavior in the G-period⁴?

Problem 14.11

Run numerical simulations of Eqs. (14.19). Prove that in order to obtain an adder, the ingredients of a size-specific (rather than constant) production rate of the division protein k_X and a reset to zero (rather than partitioning in half in the two daughter cells) of the division factor X turn out to be essential.

Problem 14.12

Rewrite the system of equations (14.20) in terms of protein fractions, either defined as protein mass fractions $\phi_i \equiv M_i/M_{\text{prot}}$ or protein number fraction $\psi_i \equiv P_i/\sum_i P_i$, where $M_{\text{prot}} = m_Q Q + m_P P + m_R R + m_X X = M - m_A A$. In both cases one has the obvious constraint $\sum \psi_i = 1 = \sum_i \phi_i$. Find the connection between ψ_i and ϕ_i . What can be generally said about the stationary composition of the proteome? How does the scenario change if degradation can be neglected?

Problem 14.13

For the mathematically curious readers, show that the model described in Box 14.E can be written in more general mathematical terms as

$$\begin{aligned} \frac{dX_i}{dt} &= f_i(\mathbf{X}); & \frac{dZ}{dt} &= h(\mathbf{X}, Z) \\ V(\mathbf{X}, Z) &= \sum_{i=1}^N v_i X_i + v_Z Z \end{aligned} \quad (14.26)$$

where V is the volume of the cell and X_i, Z its chemical constituents. Identify the functions f_i s and h . Show that the f_i s satisfy the property of homogeneity, $f_i(\beta \mathbf{X}) = \beta f_i(\mathbf{X})$. The predictions of this model have been studied in the wider framework of dynamical systems theory [72, 73].

Problem 14.14

By directly integrating Eq. (14.19), derive the following expression for the threshold number of division proteins $X_{th} \equiv X(\tau_d)$

$$X(t) = \frac{k_X s_0}{\lambda + \frac{d_X}{m_X}} \left(2^{\frac{t}{\tau_d}} - 2^{-\frac{d_X}{m_X \lambda} \frac{t}{\tau_d}} \right) \implies X_{th} = \frac{k_X}{\lambda + \frac{d_X}{m_X}} \left(s_d - s_0 2^{-\frac{d_X}{m_X \lambda}} \right). \quad (14.27)$$

⁴Note that the adder behavior can be recovered introducing asymmetric divisions [34]

Recommended readings

- Osella M, Tans SJ, Cosentino Lagomarsino M. (2017). Step by step, cell by cell: Quantification of the bacterial cell cycle. *Trends Microbiol* 25(4):250-256. doi: [10.1016/j.tim.2016.12.005](https://doi.org/10.1016/j.tim.2016.12.005).
- Willis L, Huang KC (2017). Sizing up the bacterial cell cycle. *Nat. Rev. Microbiol.* 15(10):606-620. doi: [10.1038/nrmicro.2017.79](https://doi.org/10.1038/nrmicro.2017.79).
- Cadart, C., Venkova, L., Recho, P. et al. (2019). The physics of cell-size regulation across timescales. *Nat. Phys.* 15, 9931004.
- Jun S, Si F, Pugatch R, Scott M. (2018). Fundamental principles in bacterial physiology-history, recent progress, and the future with focus on cell size control: a review. *Rep. Prog. Phys.* 81(5):056601. doi: [10.1088/1361-6633/aaa628](https://doi.org/10.1088/1361-6633/aaa628).
- Serbanescu D, Ojkic N, Banerjee S. (2021). Cellular resource allocation strategies for cell size and shape control in bacteria. *FEBS J.* doi: [10.1111/febs.16234](https://doi.org/10.1111/febs.16234).
- Amir A, Männik J, Woldringh CL, Zaritsky A. (2019). Editorial: The bacterial cell: Coupling between growth, nucleoid replication, cell division, and shape Volume 2. *Front. Microbiol.* 4;10:2056. doi: [10.3389/fmicb.2019.02056](https://doi.org/10.3389/fmicb.2019.02056).
- Kleckner NE, Chatzi K, White MA, Fisher JK, Stouf M. (2018). Coordination of Growth, Chromosome Replication/Segregation, and Cell Division in *E. coli*. *Front. Microbiol.* 9:1469. doi: [10.3389/fmicb.2018.01469](https://doi.org/10.3389/fmicb.2018.01469).

Appendix sections

14.8. Equations for birth size

Here we derive the dynamic equations of the birth size q_0^i across generations (indexed by i) in the discrete-time formalism. We define $\langle q_0 \rangle_\alpha$ as the average value of q_0 , and the log size deviation $\delta q_0^i := q_0^i - \langle q_0 \rangle_\alpha$. The dynamics for the log-size deviation takes the form

$$\delta q_0^{i+1} = g(\delta q_0^i, \alpha) + \zeta^i(\delta q_0^i, \alpha) , \quad (14.28)$$

where $\zeta^i(\delta q_0^i, \alpha)$ is a random variable with zero mean. This equation has the same degree of generality of Eq. (14.8) and can express any arbitrary division control model (or equivalently any shapes of the hazard rate function). In order to make further mathematical (and biological) progress, we need to simplify the equation and make the comparison with data possible. There are several possible choices. In the following, for simplicity, we first neglect the fluctuation of the growth rate α . Assume that the size at birth is the only variable influencing cell division ($g(\cdot)$ is a function of δq_0^i only) will allow us to introduce a linear-response framework. We will then describe how to consider the heterogeneity of multiple growth parameters.

The main empirical observation that comes to our help is the fact that the coefficient of variation of q_0^i is small (typically around 0.15) [2, 10, 20, 17, 19]. The small value of the coefficient of variation strongly suggests the possibility of Taylor-expanding the function $g(\delta q_0^i)$ around $\delta q_0^i = 0$ [20]. In this limit, the function $g(\delta q_0^i)$ is approximately linear and the random variable $\zeta^i(\delta q_0^i, \alpha)$ can be well approximated by a Gaussian random variable with zero mean and constant variance [19]. The resulting equation reads

$$\delta q_0^{i+1} = (1 - \lambda)\delta q_0^i + \sigma \xi^i , \quad (14.29)$$

where ξ^i is a Gaussian random variable with zero mean and unit variance. The two parameters λ and σ encode, respectively, the relevant information about the mechanism of size control and the level of stochasticity. The

parameter σ simply corresponds to $\zeta^i(0, \alpha)$. The parameter λ , which quantifies the strength of size control, has a direct relationship with the mechanism at its origin. It is defined as $\lambda = 1 - g'(0, \alpha)$. For instance, the sizer corresponds to $\lambda = 1$ and an adder to $\lambda = 1/2$. The case $\lambda = 0$ does not lead to a stationary process and corresponds to a timer. Consequently, this parameter can easily be inferred from the plots in Figure ??.

Eq. (14.29) can be solved analytically [19]. In particular one can show that the conditional probability of observing a log-size deviation δq_0^i from the average at generation i given a deviation at generation 0, is a Gaussian with mean

$$\langle \delta q_0^i \rangle_{\delta q_0^0} = (1 - \lambda)^i \delta q_0^0. \quad (14.30)$$

This result clearly shows how different mechanisms correspond to different strengths of cell-size homeostasis, leading to fluctuations persisting across a different number of generations. For a sizer, $\lambda = 1$, the expected deviation of the daughter cell is independent of the mother cell fluctuations. A timer, with $\lambda = 0$, does not lead to homeostasis, as the expected deviation of size at birth of a daughter cell is the same as the deviation of the mother. The adder, $\lambda = 1/2$, leads on average to a halving of the size at birth deviation at each generation, as approximately observed in experiments [10].

One can generalize the linear-response framework to consider fluctuations of different growth parameters [21]. In general, one can assume that the size at birth of the daughter cell depends on both size at birth of the mother and her individual growth rate fluctuations.

$$\delta q_0^{i+1} = (1 - \lambda_{qq}) \delta q_0^i - \lambda_{q\alpha} \delta \alpha^i + \xi_q^i. \quad (14.31)$$

Along the same lines, one can assume that the growth rate fluctuations obey a similar equation

$$\delta \alpha^{i+1} = -\lambda_{\alpha q} \delta q_0^i - \lambda_{\alpha\alpha} \delta \alpha^i + \xi_\alpha^i. \quad (14.32)$$

This kind of equation can be written in multiple forms, *i.e.* including multiple variables. For example, one can write an equation explicitly for the elongation rate between divisions $\delta G := \delta q_0^{i+1} - \delta q_0^i$ or for the division time. Since the linear-response equations assume that the fluctuations around the means of these variables are small, all these choices turn out to be mathematically equivalent. This is also the reason why the different plots in Figure ?? are equivalent. While a linear dependency of growth rate α and division time τ_d on (log-)size at birth q_0 would induce a non linear dependency of the elongation $G = \alpha \tau_d$ on the initial size, such non-linearities can be neglected in the limit of small fluctuations, leading always to linear dependencies [20, 21].

The values of the parameters λ_{ab} can be easily inferred using the standard tools of linear regression. Notably, the best (maximum likelihood) estimates of these parameters can be directly obtained from the variable covariances [19, 21]. For instance, $\langle \delta q^{i+1} \delta q^i \rangle = \lambda_{qq} \sigma_q^2 + \lambda_{q\alpha} \langle \delta \alpha^i \delta q^i \rangle$. By writing the expressions for other correlations (e.g., $\langle \delta q^{i+1} \delta \alpha^i \rangle$ or $\langle \delta \alpha^{i+1} \delta q^{i+1} \rangle$) one can map the coefficient λ_{ab} with the measured covariances.

14.9. Growth laws

Growth laws and trade-offs between protein sectors. Prototypical predictions are the so-called "growth laws", general quantitative relationships linking proteome composition and rates of cellular processes. The reason why relationships of the kind $\lambda = \lambda(\phi_R, \phi_X, \dots)$ and $k_X(\phi_R, \phi_X, \dots)$ naturally emerge in the framework is due to cell growth and division rates being coupled to proteome allocation dynamics.

Growth law for the ribosome sector. For example, the first growth law, stating that the ribosome mass fraction increases linearly with the nutrient-imposed growth rate, that is $\lambda = \lambda(\phi_R) = \mathcal{K}(\phi_R - \phi_R^{min})$, is obtained straightforwardly by noting that upon differentiation of Eq. (14.21) with respect to time and substitution of Eq. (14.19) and

Eq. (14.20) one finds the dynamical relation $\lambda(t) = \frac{k_n P(t)}{M}$, which at equilibrium reads (neglecting degradation)

$$\lambda^* = \frac{k_n P^*}{M} = \frac{ak_t R^* f_a}{M} = \frac{ak_t}{m_R} \frac{M_{prot}}{M} (\phi_R - \phi_R^{min}), \quad (14.33)$$

since at equilibrium the amino-acid import flux $k_n P^*$ matches the biosynthesis flux $ak_t R^* f_a$ ($dA/dt = 0$ in absence of degradation). Note that we have used the definitions $\phi_i \equiv (m_i P_i)/M_{prot} = (m_i P_i)/(M - M_a)$ and $Rf_a = R^{active} = R - R^{inactive}$ and we have identified $\phi_R^{inactive} = \phi_R^{min}$.

Trade-Offs between Ribosomes and Division Protein Synthesis. Following Refs. [59, 60], we re-write Eq. (14.33) as $k_n = \frac{ak_t}{m_R} m_P \frac{\phi_R - \phi_R^{min}}{\phi_P}$ and use the constraint $\phi_R^{max} = 1 - \phi_Q = \phi_R + \phi_P + \phi_X$ to obtain

$$\phi_X = -\frac{K_n + K_t}{K_n} \phi_R + \frac{K_t \phi_R^{min} + K_n \phi_R^{max}}{K_n}, \quad (14.34)$$

where $K_n \equiv k_n/m_P$ ($[K_n] = [T]^{-1}$) and $K_t \equiv ak_t/m_R$ ($[K_t] = [T]^{-1}$). Eq. (14.34) shows a negative correlation between the ribosome and division sectors under nutrient or translational perturbations, in agreement with recent published data [74]. Also, since the rates of growth and division protein synthesis are respectively proportional to the ribosome and the division sector, this negative correlation reflects a trade-offs between allocating ribosomal resources towards growth or division (see Fig.1F in Ref. [59]).

Growth law for the division sector. So, the larger the fraction of ribosomes making division proteins the smaller the fraction of ribosomes making ribosomes. In other words, there is a negative correlation between the growth rate and the division protein sector. Indeed, the ribosome sector is related to the growth rate via the first growth law $\phi_R = \frac{M\lambda}{M_{prot}K_t} + \phi_R^{min}$, but it is also related to ϕ_X via Eq. (14.34) $\phi_R = \frac{K_t \phi_R^{min} + K_n \phi_R^{max}}{K_n + K_t} - \frac{K_n}{K_n + K_t} \phi_X$. Equating the two terms yields

$$\lambda = \frac{K_n K_t}{K_n + K_t} \frac{M_{prot}}{M} (\phi_R^{max} - \phi_R^{min} - \phi_X), \quad (14.35)$$

which is Eq. (9) in Ref. [59].

We now discuss how two known steady-growth size-related behaviors emerge in the unified framework from the interplay between cell growth and cell division.

Adder mechanism. As we discussed, *E. coli* cells regulate their size by adding a constant volume between consecutive cell divisions (adder mechanism). In a previous problem, we investigated with numerical simulations the range of validity of this property. In the following one, we instead show analytically that the adder property is naturally embedded in the unified framework.

It can be seen then that whenever $\lambda \gg d_X/m_X$ (e.g. fast growth conditions), $\Delta s_{1cycle} \approx \frac{\lambda}{k_X} X_{th} = \text{const}$ which is the adder property. Notably, in increasingly slower growth conditions, where degradation becomes with the growth rate, deviations from the adder are predicted, up to the point $\lambda \ll d_X/m_X$ where $s_d \approx X_{th} d_X / (k_X m_X) = \text{const}$.

“SchaechterMaaloeKjeldgaard” (SMK) growth law. According to this law, the population-averaged cellular size scales with growth rate in an approximately exponential fashion [75]. Interestingly, deviations from the exponential trend have recently been reported, particularly at slow growth, leading to a different proposition [35]. Notably, deviations from this law are accounted in our framework. Indeed, in an exponentially expanding population the average cell size can be expressed as $\langle s \rangle = 2 \log 2 \langle s_0 \rangle$ [2], which, combined with Eq. (14.27) and $\langle s_d \rangle = 2 \langle s_0 \rangle$ leads to

$$\langle s \rangle = \frac{\lambda + \frac{d_X}{m_X}}{\tilde{k}_X \left(2 - 2^{-\frac{d_X}{m_X \lambda}} \right)} \quad (14.36)$$

where, following Ref. [59], we have defined $\tilde{k}_X \equiv k_X / (2 \log 2 X_{th})$. Note that since $\lambda \propto \phi_R$ and $k_X \propto -\phi_R$ the average cell size increases with ribosome abundance, a trend observed in experiments. Notably, upon determining

the model parameters and making full explicit the growth rate dependence, the authors in Ref. [59] with no further fitting showed that Eq. (14.36) recapitulates the experimental data [35, 59], a remarkable achievement of the unified framework.

Non-steady relationships. Finally, we contextualize within the unified framework some predictions of a model recently proposed to unify cell division and growth in *non-steady* growth conditions [48]. As we saw, although there is consensus on an inter-division adder at the phenomenological level, the mechanisms regulating cell division dynamics in the bacterium *E. coli* are still widely debated. In particular several mechanistic models based on different mechanisms for division control were proposed for the adder [42, 76, 33, 32]. In order to help selecting different scenarios, experiments beyond steady-state growth help comparing the specific causal relationships underlying different models with data. Following this philosophy, and aiming to shed more light on cell division dynamics, Panlilio et al. [48] ran multiple long-term *E. coli* microfluidics experiments jointly monitoring size-division dynamics and reporters of ribosomal and constitutive genes through nutritional up-shifts. The fluorescent reporters can be seen as proxies for the dynamics of the *R* and *P* sectors during the shift. Remarkably, in their experiments they observed highly-complex multiple-timescale dynamics in different cell-division variables (particularly inter-division time, division rate, added volume and added-to-initial volume ratio) during the nutritional up-shift. Notably, in spite of this complex dynamics, they found the division control strategy to be unaffected by the shift. The transient observed division dynamics in their shift data falsifies several scenarios, such as the Harris-Theoriot septum-limited division and the classic scenario of replication-limited division. Instead, the authors found that a threshold accumulation model such as the one described by Eq. (14.19) could not be falsified,

$$\frac{ds(t)}{dt} = \alpha(t)s(t) \qquad \frac{dN(t)}{dt} = r_X(t)s(t) . \quad (14.37)$$

This is the usual scenario where a *constitutive* *X*-sector protein accumulates to a threshold value N^* and at that point triggers cell division. The regulation of cell division from a constitutive sector is coherent with the observation that ppGpp is a cell size and cell division regulator [77]. These results are also in line with independent conclusions based on steady-state data [60, 33, 47] and isolate FtsZ as a likely candidate cell-division trigger, although the previous section has clarified how the complexity of the decision to divide is likely higher than described by the chromosome-agnostic cell-division models that are used in integrated frameworks. Future efforts will have to integrate this complexity in a description that also accounts for the interplay of different processes relevant for cell cycle progression with cell growth.

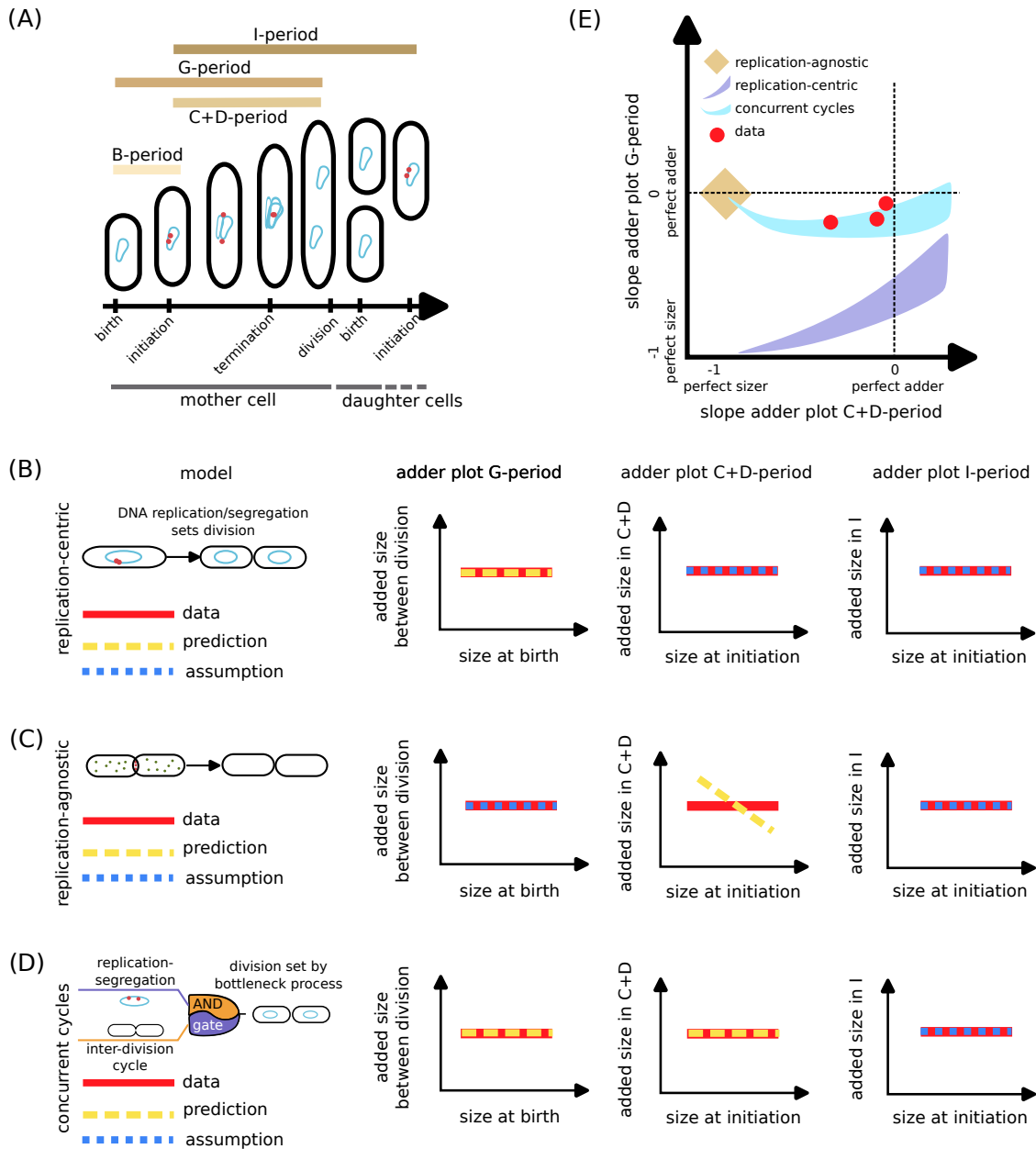
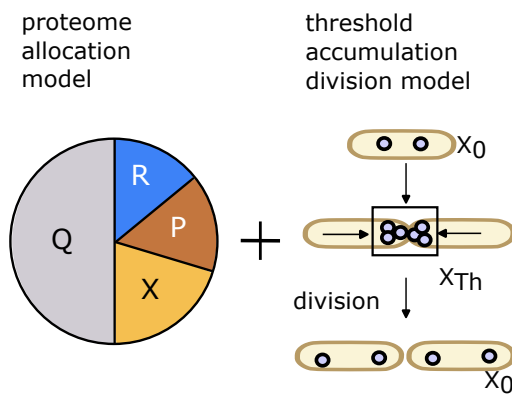


Figure 14.3: Comparison of different cell-cycle models including chromosome sub-periods proposed in the literature for *E. coli* – (A) The DNA replication-segregation cycle divides of the cell cycle into sub-periods. The B-period is the period between cell birth and initiation of DNA replication; the C-period is the period needed for completing DNA replication; and the D-period is the period between the termination of DNA replication and cell division. Finally, the I-period is the period between two consecutive initiations of DNA replication, which usually spans two generations. (B) Scheme of the ‘replication-centric class of models in which DNA replication-segregation sets division (first column). These models usually assume that the CD and the I periods are adders (blue lines in the third and fourth column, respectively), in agreement with data (red lines in the same panels). The G-period correlation pattern is a prediction of the model in general agreement with data (yellow vs red lines in the second column). (C) Schematic for the ‘replication-agnostic class of models in which a process starting at cell birth drive division (first column). These models assume the G and I periods to be adders (blue lines in the second and fourth panels, respectively). The C+D period correlation pattern is a prediction of this model which does not agree with the available data (yellow vs red lines in the third panel). (D) Schematic for the ‘concurrent cycles class of models in which two processes compete to set division through an AND gate (first column). These models assume the I periods to be an adder (blue lines in the fourth column) and using additional parameters predict both adders in the G and C+D periods (yellow lines in the second and third column). (E) Plotting the slope of the G versus the C+D-period allows to compare the different models with data. Schematic similar Figure 4 in [23].

(A) Unified coarse grained whole-cell model



(B) Model predictions

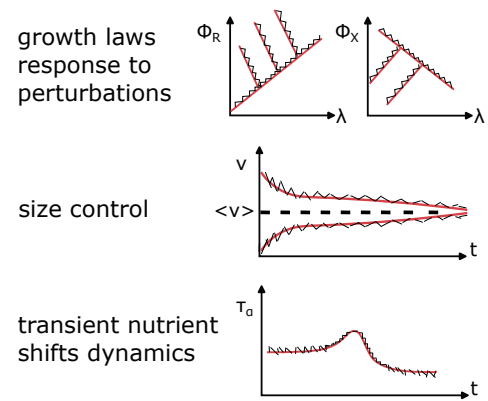


Figure 14.4: Ingredients and predictions of modeling frameworks integrating sector models with cell-division control – (A) The framework unifies growth and cell division by extending the standard proteome allocation model to include a division sector X , implementing a threshold-accumulation process setting the decision to divide. (B) The model is naturally suited to uncover general relationships and growth laws involving proteome composition and growth rate, as well as trade-offs between different proteome sectors. The inclusion of a division protein sector X regulating cell division allows the model to make predictions on cell size control and study the transient dynamics in nutrient shifts.

Bibliography

- [1] Matteo Osella, Sander J Tans, and Marco Cosentino Lagomarsino. Step by step, cell by cell: Quantification of the bacterial cell cycle. *Trends in microbiology*, 25:250–256, Apr 2017. ISSN 1878-4380. doi: 10.1016/j.tim.2016.12.005.
- [2] Suckjoon Jun, Fangwei Si, Rami Pugatch, and Matthew Scott. Fundamental principles in bacterial physiology - history, recent progress, and the future with focus on cell size control: A review. *Reports on progress in physics. Physical Society (Great Britain)*, 81(5):056601, May 2018. ISSN 0034-4885. doi: 10.1088/1361-6633/aaa628.
- [3] Lisa Willis and Kerwyn Casey Huang. Sizing up the bacterial cell cycle. *Nature Reviews Microbiology*, 15(10): 606–620, 2017.
- [4] Clotilde Cadart, Larisa Venkova, Pierre Recho, Marco Cosentino Lagomarsino, and Matthieu Piel. The physics of cell-size regulation across timescales. *Nature Physics*, 15(10):993–1004, October 2019. ISSN 1745-2481. doi: 10.1038/s41567-019-0629-y. Number: 10 Publisher: Nature Publishing Group.
- [5] Enno R. Oldewurtel, Yuki Kitahara, and Sven van Teeffelen. Robust surface-to-mass coupling and turgor-dependent cell width determine bacterial dry-mass density. *Proceedings of the National Academy of Sciences of the United States of America*, 118, August 2021. ISSN 1091-6490. doi: 10.1073/pnas.2021416118.
- [6] Ping Wang, Lydia Robert, James Pelletier, Wei Lien Dang, Francois Taddei, Andrew Wright, and Suckjoon Jun. Robust growth of *Escherichia coli*. *Current biology*, 20(12):1099–1103, 2010.
- [7] Matteo Osella, Eileen Nugent, and Marco Cosentino Lagomarsino. Concerted control of *Escherichia coli* cell division. *Proc. Natl. Acad. Sci. (U.S.A.)*, 111(9):3431–5, 2014.
- [8] Jan M. Skotheim. Cell growth and cell cycle control. *Mol. Biol. Cell*, 24(6):678, 2013.
- [9] Manuel Campos, Ivan V. Surovtsev, Setsu Kato, Ahmad Paintdakhi, Bruno Beltran, Sarah E. Ebmeier, and Christine Jacobs-Wagner. A constant size extension drives bacterial cell size homeostasis. *Cell*, 159(6):1433–46, Dec 2014. doi: 10.1016/j.cell.2014.11.022.
- [10] Sattar Taheri-Araghi, Serena Bradde, John T Sauls, Norbert S Hill, Petra A Levin, Johan Paulsson, Massimo Vergassola, and Suckjoon Jun. Cell-size control and homeostasis in bacteria. *Current biology : CB*, 25:385–391, Feb 2015. ISSN 1879-0445. doi: 10.1016/j.cub.2014.12.009.
- [11] DJF Davis. An analysis of some failure data. *Journal of the American Statistical Association*, 47(258):113–150, 1952.
- [12] John J Tyson and Kenneth B Hannsgen. Global asymptotic stability of the size distribution in probabilistic models of the cell cycle. *Journal of mathematical biology*, 22(1):61–8, 1985.
- [13] T G Clark, M J Bradburn, S B Love, and D G Altman. Survival analysis part I: Basic concepts and first analyses. *British Journal of Cancer*, 89(2):232–238, July 2003. doi: 10.1038/sj.bjc.6601118.
- [14] Federico Bassetti, Ilenia Epifani, and Lucia Ladelli. Cox Markov models for estimating single cell growth. *Electronic Journal of Statistics*, 11(2):2931 – 2977, 2017. doi: 10.1214/17-EJS1306.

- [15] Martijn Wehrens, Dmitry Ershov, Rutger Rozendaal, Noreen Walker, Daniel Schultz, Roy Kishony, Petra Anne Levin, and Sander J. Tans. Size laws and division ring dynamics in filamentous *Escherichia coli* cells. *Current Biology*, 28(6):972–979.e5, March 2018. doi: 10.1016/j.cub.2018.02.006.
- [16] Andrea Giometto, Florian Altermatt, Francesco Carrara, Amos Maritan, and Andrea Rinaldo. Scaling body size fluctuations. *Proc. Natl. Acad. Sci. (U.S.A.)*, 110(12):4646–50, Mar 2013.
- [17] Andrew S. Kennard, Matteo Osella, Avelino Javier, Jacopo Grilli, Philippe Nghe, Sander J. Tans, Pietro Cicuta, and Marco Cosentino Lagomarsino. Individuality and universality in the growth-division laws of single *E. coli* cells. *Phys Rev E*, 93(1):012408, Jan 2016. doi: 10.1103/PhysRevE.93.012408.
- [18] Srividya Iyer-Biswas, Gavin E Crooks, Norbert F Scherer, and Aaron R Dinner. Universality in stochastic exponential growth. *Phys. Rev. Lett.*, 113(2):028101, 2014.
- [19] Jacopo Grilli, Matteo Osella, Andrew S. Kennard, and Marco Cosentino Lagomarsino. Relevant parameters in models of cell division control. *Physical Review E*, 95(3):032411, 2017. doi: 10.1103/PhysRevE.95.032411.
- [20] Ariel Amir. Cell size regulation in bacteria. *Phys. Rev. Lett.*, 112(20):208102, 2014. doi: 10.1103/PhysRevLett.112.208102.
- [21] Jacopo Grilli, Clotilde Cadart, Gabriele Micali, Matteo Osella, and Marco Cosentino Lagomarsino. The empirical fluctuation pattern of *E. coli* division control. *Frontiers in Microbiology*, 9:1541, 2018. ISSN 1664-302X. doi: 10.3389/fmicb.2018.01541.
- [22] M Schaechter, O Maaløe, and N O Kjeldgaard. Dependency on medium and temperature of cell size and chemical composition during balanced grown of *Salmonella typhimurium*. *J. Gen. Microbiol.*, 19(3):592–606, Dec 1958.
- [23] Alexandra Colin, Gabriele Micali, Louis Faure, Marco Lagomarsino, and Sven van Teeffelen. Two different cell-cycle processes determine the timing of cell division in *Escherichia coli*. *eLife*, 10, 2021. doi: 10.7554/eLife.67495.
- [24] M Meselson and F W Stahl. The replication of DNA in *Escherichia coli*. *Proceedings of the National Academy of Sciences of the United States of America*, 44:671–682, Jul 1958. ISSN 0027-8424.
- [25] S Cooper and C E Helmstetter. Chromosome replication and the division cycle of *Escherichia coli* B/r. *J. Mol. Biol.*, 31(3):519–40, 1968.
- [26] David Bates and Nancy Kleckner. Chromosome and replisome dynamics in *E. coli*: loss of sister cohesion triggers global chromosome movement and mediates chromosome segregation. *Cell*, 121(6):899–911, Jun 2005. doi: 10.1016/j.cell.2005.04.013.
- [27] Nancy E. Kleckner, Katerina Chatzi, Martin A. White, Jay K. Fisher, and Mathieu Stouf. Coordination of growth, chromosome replication/segregation, and cell division in *E. coli*. *Frontiers in Microbiology*, 9:1469, 2018. ISSN 1664-302X. doi: 10.3389/fmicb.2018.01469.
- [28] David Magnan and David Bates. Regulation of DNA replication initiation by chromosome structure. *Journal of bacteriology*, 197(21):3370–3377, 2015.
- [29] Ole Michelsen, M Joost Teixeira de Mattos, Peter Ruhdal Jensen, and Flemming G Hansen. Precise determinations of C and D periods by flow cytometry in *Escherichia coli* K-12 and B/r. *Microbiology*, 149(4):1001–10, April 2003. ISSN 1350-0872. doi: 10.1099/mic.0.26058-0.
- [30] Matthew A A. Grant, Chiara Saggioro, Ulisse Ferrari, Bruno Bassetti, Bianca Sclavi, and Marco Cosentino Lagomarsino. DnaA and the timing of chromosome replication in *Escherichia coli* as a function of growth rate. *BMC Syst Biol*, 5:201, 2011. doi: 10.1186/1752-0509-5-201.

- [31] Aileen Adiciptaningrum, Matteo Osella, M Charl Moolman, Marco Cosentino Lagomarsino, and Sander J Tans. Stochasticity and homeostasis in the *E. coli* replication and division cycle. *Scientific reports*, 5:18261, Dec 2015. ISSN 2045-2322. doi: 10.1038/srep18261.
- [32] Mats Wallden, David Fange, Ebba Gregorsson Lundius, Özden Baltekin, and Johan Elf. The synchronization of replication and division cycles in individual *E. coli* cells. *Cell*, 166(3):729–739, 2016.
- [33] Fangwei Si, Guillaume Le Treut, John T. Sauls, Stephen Vadia, Petra Anne Levin, and Suckjoon Jun. Mechanistic origin of cell-size control and homeostasis in bacteria. *Current Biology*, 29(11):1760–1770.e7, June 2019. ISSN 0960-9822. doi: 10.1016/j.cub.2019.04.062. Publisher: Elsevier.
- [34] Guillaume Witz, Erik van Nimwegen, and Thomas Julou. Initiation of chromosome replication controls both division and replication cycles in *E. coli* through a double-adder mechanism. *Elife*, 8:e48063, 2019.
- [35] Hai Zheng, Yang Bai, Meiling Jiang, Taku A Tokuyasu, Xiongliang Huang, Fajun Zhong, Yuqian Wu, Xiongfei Fu, Nancy Kleckner, Terence Hwa, et al. General quantitative relations linking cell growth and the cell cycle in *Escherichia coli*. *Nature Microbiology*, 5(8):995–1001, 2020.
- [36] Hai Zheng, Po-Yi Ho, Meiling Jiang, Bin Tang, Weirong Liu, Dengjin Li, Xuefeng Yu, Nancy E Kleckner, Ariel Amir, and Chenli Liu. Interrogating the *Escherichia coli* cell cycle by cell dimension perturbations. *Proceedings of the National Academy of Sciences of the United States of America*, 113:15000–15005, Dec 2016. ISSN 1091-6490. doi: 10.1073/pnas.1617932114.
- [37] Fangwei Si, Dongyang Li, Sarah E Cox, John T Sauls, Omid Azizi, Cindy Sou, Amy B Schwartz, Michael J Erickstad, Yonggun Jun, Xintian Li, and Suckjoon Jun. Invariance of initiation mass and predictability of cell size in *Escherichia coli*. *Current biology : CB*, 27:1278–1287, May 2017. ISSN 1879-0445. doi: 10.1016/j.cub.2017.03.022.
- [38] Gabriele Micali, Jacopo Grilli, Jacopo Marchi, Matteo Osella, and Marco Cosentino Lagomarsino. Dissecting the control mechanisms for DNA replication and cell division in *E. coli*. *Cell Reports*, 25(3):761–771.e4, October 2018. ISSN 2211-1247. doi: 10.1016/j.celrep.2018.09.061.
- [39] Michelle M. Logsdon, Po-Yi Ho, Kadamba Papavinasasundaram, Kirill Richardson, Murat Cokol, Christopher M. Sassetti, Ariel Amir, and Bree B. Aldridge. A parallel adder coordinates mycobacterial cell-cycle progression and cell-size homeostasis in the context of asymmetric growth and organization. *Current Biology*, 2017.
- [40] Gabriele Micali, Jacopo Grilli, Matteo Osella, and Marco Cosentino Lagomarsino. Concurrent processes set *E. coli* cell division. *Science Advances*, 4(11):eaau3324, November 2018. ISSN 2375-2548. doi: 10.1126/sciadv.aau3324. Publisher: American Association for the Advancement of Science Section: Research Article.
- [41] Leigh K Harris and Julie A Theriot. Surface area to volume ratio: a natural variable for bacterial morphogenesis. *Trends in microbiology*, 26(10):815–832, 2018.
- [42] Leigh K Harris and Julie A Theriot. Relative rates of surface and volume synthesis set bacterial cell size. *Cell*, 165(6):1479–1492, 2016.
- [43] P Ho and A Amir. Simultaneous regulation of cell size and chromosome replication in bacteria. *Front. Microbiol.* 6: 662, 2015.
- [44] Guillaume Witz, Thomas Julou, and Erik van Nimwegen. Response to comment on initiation of chromosome replication controls both division and replication cycles in *E. coli* through a double-adder mechanism. *bioRxiv*, page 2020.08.04.227694, August 2020. doi: 10.1101/2020.08.04.227694. Publisher: Cold Spring Harbor Laboratory Section: Contradictory Results.

- [45] William D Donachie. Relationship between cell size and time of initiation of DNA replication. *Nature*, 219: 1077–9, 1968.
- [46] Michelle M. Logsdon and Bree B. Aldridge. Stable regulation of cell cycle events in mycobacteria: Insights from inherently heterogeneous bacterial populations. *Frontiers in Microbiology*, 9, 2018. ISSN 1664-302X. doi: 10.3389/fmicb.2018.00514. Publisher: Frontiers.
- [47] Nikola Ojkic, Diana Serbanescu, and Shiladitya Banerjee. Surface-to-volume scaling and aspect ratio preservation in rod-shaped bacteria. *eLife*, 8:e47033, August 2019. ISSN 2050-084X. doi: 10.7554/eLife.47033. Publisher: eLife Sciences Publications, Ltd.
- [48] Mia Panlilio, Jacopo Grilli, Giorgio Tallarico, Ilaria Iuliani, Bianca Sclavi, Pietro Cicuta, and Marco Cosentino Lagomarsino. Threshold accumulation of a constitutive protein explains E. coli cell-division behavior in nutrient upshifts. *Proceedings of the National Academy of Sciences*, 118(18):e2016391118, 2021.
- [49] Guillaume Le Treut, Fangwei Si, Dongyang Li, and Suckjoon Jun. Comment on initiation of chromosome replication controls both division and replication cycles in E. coli through a double-adder mechanism. *bioRxiv*, page 2020.05.08.084376, May 2020. doi: 10.1101/2020.05.08.084376. Publisher: Cold Spring Harbor Laboratory Section: Contradictory Results.
- [50] Guillaume Le Treut, Fangwei Si, Dongyang Li, and Suckjoon Jun. Quantitative examination of five stochastic cell-cycle and cell-size control models for Escherichia coli and Bacillus subtilis. *Frontiers in microbiology*, page 3278, 2021.
- [51] Sriram Tiruvadi-Krishnan, Jaana Männik, Prathitha Kar, Jie Lin, Ariel Amir, and Jaan Männik. Coupling between DNA replication, segregation, and the onset of constriction in escherichia coli. *Cell reports*, 38(12): 110539, 2022.
- [52] The Economic Cell Collective, editor. *Economic Principles in Cell Biology*. Free online book, 2023. doi: 10.5281/zenodo.8156386.
- [53] Frank J Bruggeman, Robert Planqué, Douwe Molenaar, and Bas Teusink. Searching for principles of microbial physiology. *FEMS Microbiology Reviews*, 44(6):821–844, 09 2020. doi: 10.1093/femsre/fuaa034.
- [54] Ariel Amir, Jaan Männik, Conrad L. Woldringh, and Arie Zaritsky. Editorial: The bacterial cell: Coupling between growth, nucleoid replication, cell division, and shape volume 2. *Frontiers in Microbiology*, 10:2056, September 2019. ISSN 1664-302X. doi: 10.3389/fmicb.2019.02056.
- [55] F. Bertaux, S. Marguerat, and V. Shahrezaei. Division rate, cell size and proteome allocation: Impact on gene expression noise and implications for the dynamics of genetic circuits. *Royal Society Open Science*, 5(3), 2018. doi: 10.1098/rsos.172234.
- [56] Itzhak Fishov, A Zaritsky, and N B Grover. On microbial states of growth. *Molecular Microbiology*, 15(5): 789–94, 1995.
- [57] Shicong Xie, Matthew Swaffer, and Jan M. Skotheim. Eukaryotic cell size control and its relation to biosynthesis and senescence. *Annual review of cell and developmental biology*, May 2022. ISSN 1530-8995. doi: 10.1146/annurev-cellbio-120219-040142.
- [58] Patrick P Dennis and Hans Bremer. Modulation of chemical composition and other parameters of the cell at different exponential growth rates. *EcoSal Plus*, 1(2), October 2008. ISSN 2324-6200. doi: 10.1128/ecosal.5.2.3.

- [59] Diana Serbanescu, Nikola Ojkic, and Shiladitya Banerjee. Nutrient-dependent trade-offs between ribosomes and division protein synthesis control bacterial cell size and growth. *Cell Reports*, 32(12):108183, 2020. ISSN 2211-1247. doi: 10.1016/j.celrep.2020.108183.
- [60] Diana Serbanescu, Nikola Ojkic, and Shiladitya Banerjee. Cellular resource allocation strategies for cell size and shape control in bacteria. *The FEBS Journal*, 2021.
- [61] François Bertaux, Julius von K  gelgen, Samuel Marguerat, and Vahid Shahrezaei. A bacterial size law revealed by a coarse-grained model of cell physiology. *PLoS Computational Biology*, 16(9), September 2020. ISSN 1553-734X. doi: 10.1371/journal.pcbi.1008245.
- [62] Parth Pratim Pandey, Harshant Singh, and Sanjay Jain. Exponential trajectories, cell size fluctuations and the adder property in bacteria follow from simple chemical dynamics and division control. *bioRxiv*, page 487504, December 2018. doi: 10.1101/487504. Publisher: Cold Spring Harbor Laboratory Section: New Results.
- [63] Niclas Nordholt, Johan H. van Heerden, and Frank J. Bruggeman. Biphasic cell-size and growth-rate homeostasis by single *Bacillus subtilis* cells. *Current Biology*, 30(12):2238–2247.e5, June 2020. doi: 10.1016/j.cub.2020.04.030.
- [64] Prathitha Kar, Sriram Tiruvadi-Krishnan, Jaana M  nnik, Jaan M  nnik, and Ariel Amir. Distinguishing different modes of growth using single-cell data. *eLife*, 10, December 2021. doi: 10.7554/elife.72565.
- [65] Alexi I. Goranov, Michael Cook, Marketa R  cicova, Giora Ben-Ari, Christian Gonzalez, Carl Hansen, Mike Tyers, and Angelika Amon. The rate of cell growth is governed by cell cycle stage. *Genes & Development*, 23(12): 1408–1422, June 2009. doi: 10.1101/gad.1777309.
- [66] Alexi I. Goranov and Angelika Amon. Growth and division—not a one-way road. *Curr Opin Cell Biol*, 22(6): 795–800, Dec 2010. doi: 10.1016/j.ceb.2010.06.004.
- [67] J.M. Mitchison. The growth of single cells. *Experimental Cell Research*, 15(1):214–221, August 1958. doi: 10.1016/0014-4827(58)90077-6.
- [68] Stephan Baumg  rtner and Iva M. Toli  c-N  rrelykke. Growth pattern of single fission yeast cells is bilinear and depends on temperature and DNA synthesis. *Biophysical Journal*, 96(10):4336–4347, May 2009. doi: 10.1016/j.bpj.2009.02.051.
- [69] Clotilde Cadart, Larisa Venkova, Matthieu Piel, and Marco Cosentino Lagomarsino. Volume growth in animal cells is cell cycle dependent and shows additive fluctuations. *eLife*, 11, January 2022. doi: 10.7554/elife.70816.
- [70] Giuseppe Facchetti, Benjamin Knapp, Ignacio Flor-Parra, Fred Chang, and Martin Howard. Reprogramming Cdr2-dependent geometry-based cell size control in fission yeast. *Current Biology*, 29(2):350–358.e4, January 2019. doi: 10.1016/j.cub.2018.12.017.
- [71] Ariel Amir. Is cell size a spandrel? *eLife*, 6, Jan 2017. ISSN 2050-084X. doi: 10.7554/eLife.22186.
- [72] Parth Pratim Pandey, Harshant Singh, and Sanjay Jain. Exponential trajectories, cell size fluctuations, and the adder property in bacteria follow from simple chemical dynamics and division control. *Physical review. E*, 101: 062406, June 2020. ISSN 2470-0053. doi: 10.1103/PhysRevE.101.062406.
- [73] Wei-Hsiang Lin, Edo Kussell, Lai-Sang Young, and Christine Jacobs-Wagner. Origin of exponential growth in nonlinear reaction networks. *Proceedings of the National Academy of Sciences of the United States of America*, 117:27795–27804, November 2020. ISSN 1091-6490. doi: 10.1073/pnas.2013061117.

- [74] Matteo Mori, Zhongge Zhang, Amir Banaei-Esfahani, Jean-Benoît Lalanne, Hiroyuki Okano, Ben C Collins, Alexander Schmidt, Olga T Schubert, Deok-Sun Lee, Gene-Wei Li, et al. From coarse to fine: the absolute *Escherichia coli* proteome under diverse growth conditions. *Molecular systems biology*, 17(5):e9536, 2021.
- [75] M. Schaechter, J. P. Williamson, J.R. Jr Hood, and A. L. Koch. Growth, cell and nuclear divisions in some bacteria. *J. Gen. Microbiol.*, 29:421–34, Nov 1962.
- [76] Markus Basan, Sheng Hui, Hiroyuki Okano, Zhongge Zhang, Yang Shen, James R. Williamson, and Terence Hwa. Overflow metabolism in *Escherichia coli* results from efficient proteome allocation. *Nature*, 528(7580): 99–104, 2015. ISSN 14764687. doi: 10.1038/nature15765.
- [77] Ferhat Büke, Jacopo Grilli, Marco Cosentino Lagomarsino, Gregory Bokinsky, and Sander J Tans. ppGpp is a bacterial cell size regulator. *Current Biology*, 32(4):870–877, 2022.